MEMORANDUM
RM-4630-PR
JANUARY 1966

THE LONGITUDINAL AND LATERAL RANGE OF HYPERSONIC GLIDE VEHICLES WITH CONSTANT BANK ANGLE

S. Y. Chen

PREPARED FOR:

UNITED STATES AIR FORCE PROJECT RAND

The RAND Corporation
SANTA MONICA • CALIFORNIA

MEMORANDUM

RM-4630-PR

JANUARY 1966

THE LONGITUDINAL AND LATERAL RANGE OF HYPERSONIC GLIDE VEHICLES WITH CONSTANT BANK ANGLE

S. Y. Chen

This research is sponsored by the United States Air Force under Project RAND—Contract No. AF 49(638)-1700—monitored by the Directorate of Operational Requirements and Development Plans, Deputy Chief of Staff, Research and Development, Hq USAF. Views or conclusions contained in this Memorandum should not be interpreted as representing the official opinion or policy of the United States Air Force.

The RAND Corporation

1700 MAIN ST • SANTA MONICA • CALIFORNIA • 90406

PREFACE

This Memorandum has been prepared as a part of a continuing study of hypersonic lifting-vehicle technology. It is an extension of previous investigations of the use of aerodynamic forces to provide lateral-range capability for glide-reentry vehicles. The closed-form solutions presented here should be of interest to designers and planners concerned with the preliminary design and capabilities of hypersonic glide vehicles.

SUMMARY

Approximate closed-form solutions for various flight conditions have been obtained to determine both the longitudinal and lateral range of hypersonic glide vehicles with constant bank angle. Results for equilibrium-glide vehicles with a constant lift-to-drag (L/D) ratio and small and slowly changing flight-path angle are presented in graphical form. Other approximate closed-form solutions are also obtained for glide reentry at very small flight-path angle, near-constant-speed glide at high altitude, constant-deceleration glide at constant altitude, and constant-deceleration glide at fixed flight-path angle.

The assumption of a very small flight-path angle ($\gamma \approx 0$) results in a smaller range prediction than does the assumption of a small and slowly changing flight-path angle ($\gamma \approx 0.01$ rad). This is especially true for prediction of the lateral range of vehicles with high lift-to-drag ratio. For a vehicle with an L/D of 3, entering at 0.98 orbital velocity and decelerating to 0.2 orbital velocity, the assumption of a very small flight-path angle results in predictions that underestimate lateral and longitudinal range by 22.6 and 22.5 percent, respectively, in comparison with the predictions based on the assumption of a small and slowly changing flight-path angle. In other words, completely neglecting the flight-path angle in the equations of motion leads to a conservative range prediction.

ACKNOWLEDGMENTS

The author wishes to thank Carl Gazley, Jr. and Fred S. Nyland for their encouragement and discussions on this problem, and Carolyn R. Huber for performing the numerical computations.

CONTENTS

BLANK PAGE

SYMBOLS

A = area

$A_1 = \gamma_e^2 + B_1 e^{-\bar{\zeta}\bar{r}_e}$

$A_2 = -1/\left(\frac{\dot{u}}{g}\cos\phi\right)$

$B_1 = D_L(\cos\phi/\bar{\zeta})$

C = constant of integration

C_D = drag coefficient

C_L = lift coefficient

D = drag force = $C_D\rho u^2 A/2$

$D_D = \rho_o u_o^2/(W/C_D A)$

$D_L = \rho_o u_o^2/(W/C_L A)$

g = acceleration due to gravity

h = altitude

h_e = entry altitude

h_i = initial altitude

L = lift force = $C_L\rho u^2 A/2$

R_E = earth's radius

$R_o = u_o^2/g$

$\bar{r}$ = dimensionless altitude, Eqs. (7)

$\bar{r}_e = h_e/(R_E + h_e) \approx h_e/R_E$

$\bar{r}_i = h_i/(R_E + h_e) \approx h_i/R_E$

S = distance along the flight path

t = time

u = flight speed at any given time

u_e = entry speed

u_i = initial speed

u_o = orbital speed at reference altitude or entry

V = velocity ratio = u/u_o, Eqs. (7)

V_e = reentry velocity ratio = u_e/u_o

V_i = initial velocity ratio = u_i/u_o

W = vehicle weight

x = downrange distance

y = siderange distance

$\bar{\alpha}$ = $\tan \bar{\varphi}/[\bar{\gamma}(\beta - 2)]$

β = $2/[\gamma(L/D) \cos \bar{\varphi}]$

γ = flight-path angle

$\bar{\gamma}$ = mean value of small and slowly changing flight-path angle

γ_e = flight-path angle at entry

γ_i = initial flight-path angle

ζ = inverse scale height

$\bar{\zeta}$ = $\zeta(R_E + h_e) \approx R_E\zeta$

λ = lateral-range angle

ρ = atmospheric density

ρ_o = reference atmospheric density

$\bar{\rho}$ = dimensionless density ratio, Eqs. (7)

$\bar{\varphi}$ = bank angle

ω = turn angle

ω_e = turn angle at entry

ω_i = initial turn angle

I. INTRODUCTION

The problem of obtaining closed-form solutions for glide-reentry vehicles has been an area of interest for many years. Since the general exact analytical solutions of the fundamental equations of motion for glide reentry are difficult to obtain, various approximations have been made by different authors for different flight conditions. For instance, the closed solutions for very small angles of inclination have been derived by Gazley.[1,2] Eggers et al. also obtained approximate closed-form solutions for small angles of inclination.[3] Chapman has developed analytical solutions for small angles of inclination and small lift-to-drag (L/D) ratios.[4] The solutions for moderate angles of inclination and medium L/D ratios were solved by Lees et al.[5] Loh has derived closed-form solutions for negative lift at small and large angles of inclination.[6] For entry at small L/D ratios and large angles of inclination, the approximate results of Arthur are available.[7] Loh later obtained a second-order approximate solution for a nonoscillatory type of entry trajectory and derived some exact analytical solutions for certain trajectory variations.[8,9] Recently, Cohen has developed the closed-form solutions for a constant-deceleration flight path.[10] Loh extended his second-order solutions to an oscillatory type of entry trajectory.[11] However, most of these results are for two-dimensional trajectories where the bank angle is zero.

The closed-form solutions for a three-dimensional trajectory at a constant and very small angle of inclination with constant bank-angle control have been obtained by Nyland.[12] This Memorandum extends Nyland's results to obtain exact closed-form solutions for equilibrium-glide path at small and slowly changing angles of inclination, as well as for some special cases where the angles of inclination are larger. A constant bank angle is assumed for both flight conditions. The results for an equilibrium-glide path at small and slowly changing angles of inclination are also shown in graphical form to provide information for preliminary-design purposes.

II. MATHEMATICAL ANALYSIS

The general equations of motion with constant bank angle in a nonrotating three-dimensional inertial coordinate system, as shown in Fig. 1, are

$$\frac{1}{g}\dot{u} = \sin\gamma - \frac{D}{W} \tag{1}$$

$$-\frac{u}{g}\dot{\gamma} = \frac{L}{W}\cos\Phi - \left(1 - \frac{u^2}{u_o^2}\right)\cos\gamma \tag{2}$$

$$\frac{u}{g}\dot{\omega}\cos\gamma = \frac{L}{W}\sin\Phi - \frac{u^2\cos^2\gamma\cos\omega\tan\lambda}{u_o^2} \tag{3}$$

where u is the speed at any given time, t is the time, γ is the flight-path angle in the vertical direction, D is the drag force, W is the vehicle weight, L is the lift force, Φ is the bank angle, u_o is the orbital speed at an entry altitude of 400,000 ft, ω is the vehicle turn angle (heading angle), and λ is the lateral-range angle. Equation (1) pertains to motion along the flight path, Eq. (2) to motion up and down the local vertical, and Eq. (3) to a direction out of the flight plane. It is assumed that the altitude region of interest is below 400,000 ft and that gravity does not change very much between sea level and 400,000 ft. It is further assumed that

$$\frac{L}{D}\sin\Phi \gg \frac{u^2\cos^2\gamma\cos\omega\tan\lambda}{u_o^2}$$

and

$$\sin\gamma \approx \gamma \qquad \cos\gamma \approx 1$$

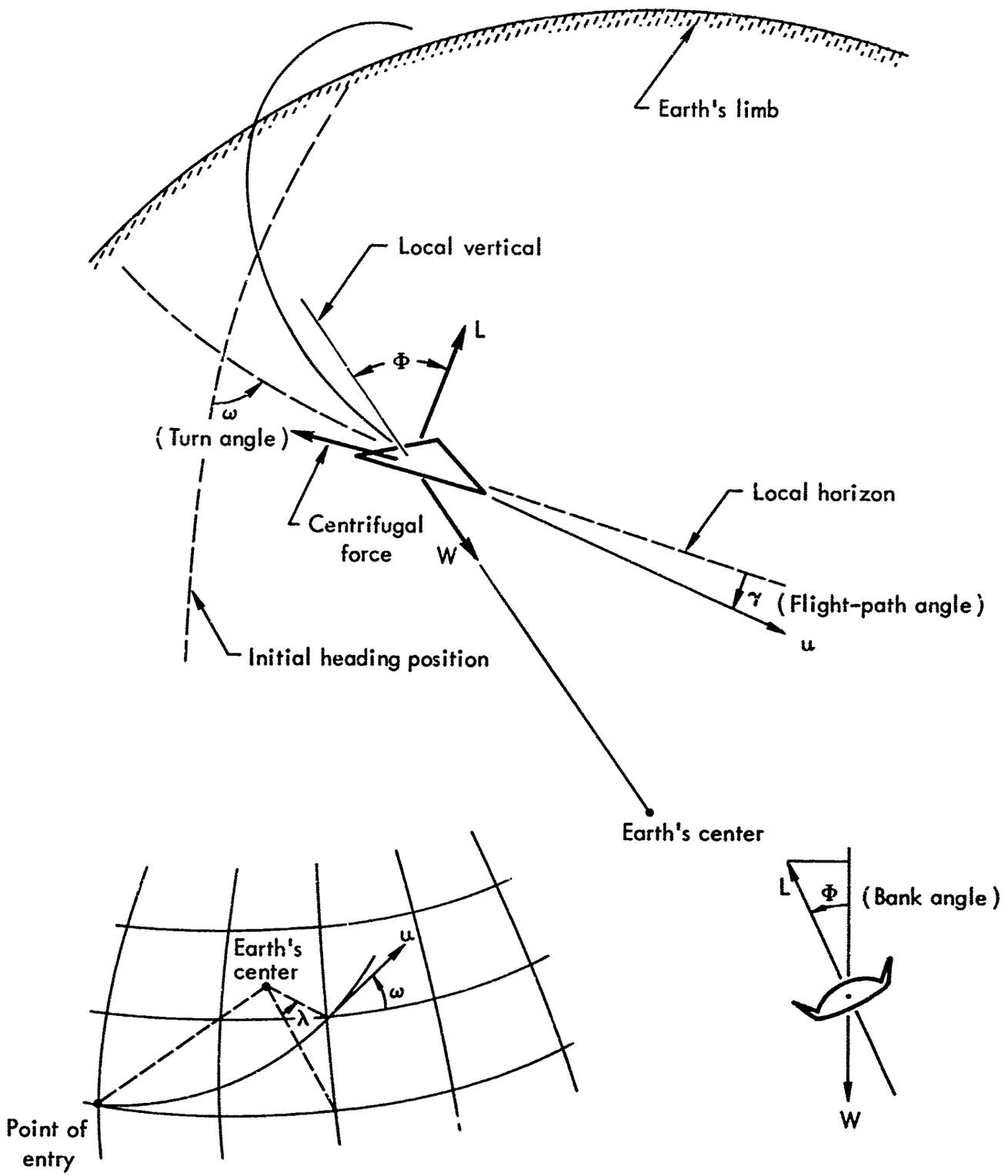

Fig. 1—Three-dimensional flight-trajectory coordinates

The first assumption indicates that the centrifugal-force component in the lateral flight plane is small in comparison with the lift component in the lateral flight plane. This assumption, which is used throughout this study, is also used by Nyland.[12] However, for constant-altitude glide at superorbital speeds, this assumption may cause an error of 30 percent for L/D = 2 in heading-angle change, as pointed out by Wang.[13] The second assumption has been relaxed for one special case, given later. With these assumptions, Eqs. (1) to (3) can be written as

$$\frac{1}{g}\dot{u} = \gamma - \frac{D}{W} \tag{4}$$

$$-\frac{u}{g}\dot{\gamma} = \frac{L}{W}\cos\tilde{\varphi} - \left(1 - \frac{u^2}{u_o^2}\right) \tag{5}$$

$$\frac{u}{g}\dot{\omega} = \frac{L}{W}\sin\tilde{\varphi} \tag{6}$$

Let

$$u = \frac{dS}{dt} \qquad dh = -\gamma dS \qquad \bar{\rho} = \frac{\rho u_o^2}{W/A}$$

$$V = \frac{u}{u_o} \qquad \bar{r} = \frac{h}{R_E + h_e} \tag{7}$$

where S is the distance along the flight path, h is the altitude, h_e is the entry altitude, and R_E is the earth's radius. These variables were introduced by Cohen, but $\bar{\rho}$ has been modified.[10] Equations (4) to (6) can then be rewritten as

$$\frac{dV^2}{d\bar{r}} - \frac{1}{\gamma} C_D \bar{\rho} V^2 = -2 \tag{8}$$

$$\frac{d\gamma^2}{d\bar{r}} = C_L\bar{\rho}\cos\Phi - 2\left(\frac{1}{V^2} - 1\right) \tag{9}$$

$$\frac{d\omega}{d\bar{r}} = -\frac{C_L\bar{\rho}}{2\gamma}\sin\Phi \tag{10}$$

where C_D and C_L are drag and lift coefficients, respectively. Equations (8) to (10) are first-order ordinary differential equations, and their general solutions are

$$V^2 = V_e^2 e^{\int_{\bar{r}_e}^{\bar{r}} \frac{C_D\bar{\rho}}{\gamma}\,d\bar{r}} + 2e^{\int \frac{C_D\bar{\rho}}{\gamma}\,d\bar{r}} \int_{\bar{r}}^{\bar{r}_e} e^{-\int \frac{C_D\bar{\rho}}{\gamma}\,d\bar{r}}\,d\bar{r} \tag{11}$$

$$\gamma^2 = \int_{\bar{r}_e}^{\bar{r}} \left(C_L\bar{\rho}\cos\Phi - \frac{2}{V^2} + 2\right)\,d\bar{r} + \gamma_e^2 \tag{12}$$

$$\omega = -\int_{\bar{r}_e}^{\bar{r}} \frac{C_L\bar{\rho}}{2\gamma}\sin\Phi\,d\bar{r} + \omega_e \tag{13}$$

where

$\bar{r}_e = h_e/(R_E + h_e)$

$V_e = u_e/u_o$

R_e = entry altitude

u_e = entry speed at h_e

γ_e = entry flight-path angle at h_e

ω_e = entry turn angle at h_e

Equations (11) and (12) have to be solved simultaneously and numerically. However, for some special reentry cases, as presented below, the solutions can be written in more simple forms.

GLIDE REENTRY TRAJECTORIES AT SMALL AND SLOWLY CHANGING FLIGHT-PATH ANGLE

One kind of atmospheric entry by lifting vehicles at small angles of inclination is an equilibrium-glide flight path, where the gravitational force is balanced by the lift force and by the centrifugal force due to the curvature of the flight path. With the assumption of a slowly changing flight-path angle, or $\gamma \approx 0$ and $|\dot{\gamma}| < \gamma$, which is also assumed by Gazley,[1] Eggers et al.,[3] and Nyland,[12] Eqs. (4) to (6) reduce to

$$\frac{1}{g}\dot{u} = \gamma - \frac{D}{W} \tag{14}$$

$$0 = \frac{L}{W}\cos\Phi - 1 - \frac{u^2}{u_o^2} \tag{15}$$

$$\frac{u}{g}\dot{\omega} = \frac{L}{W}\sin\Phi \tag{16}$$

Gazley[1] and Eggers et al.[3] solved Eqs. (14) and (15) for the two-dimensional case, where $\Phi = 0$, by assuming $\gamma \approx 0$; while Nyland[12] obtained solutions for the three-dimensional case, solving Eqs. (14) and (15) by assuming $\gamma \approx 0$ and Φ = constant. Although it is assumed here that Φ = constant, γ is considered in Eq. (14) as small but not negligible. In terms of the new variables V and $\bar{r}$, as introduced in Eq. (7), Eqs. (14) to (16) can be rewritten as

$$\frac{C_D\bar{\rho}}{2}V^2 = \gamma + \frac{\gamma}{2}\frac{dV^2}{d\bar{r}} \tag{14a}$$

$$\frac{C_L\bar{\rho}}{2}V^2\cos\Phi = 1 - V^2 \tag{15a}$$

$$\frac{C_L\bar{\rho}}{2}V^2\sin\Phi = -\gamma V^2\frac{d\omega}{d\bar{r}} \tag{16a}$$

Dividing Eq. (14a) by Eq. (15a) yields

$$\frac{dV^2}{d\bar{r}} + \beta V^2 = \beta - 2 \tag{17}$$

where

$$\beta = \frac{2}{\gamma \frac{C_L}{C_D} \cos \bar{\Phi}} = \frac{2}{\gamma \frac{L}{D} \cos \bar{\Phi}}$$

and is a function of γ, L/D, and $\bar{\Phi}$. The solution of Eq. (17) is

$$V^2 = e^{-\int \beta \, d\bar{r}} \int e^{\int \beta \, d\bar{r}} (\beta - 2) \, d\bar{r} + Ce^{-\int \beta \, d\bar{r}} \tag{18}$$

where C is a constant of integration. The initial condition is $u = u_e$ at $h = h_e$, or $V = V_e$ at $\bar{r} = \bar{r}_e$. Then Eq. (18) can be rewritten as

$$V^2 = V_e e^{\int_{\bar{r}}^{\bar{r}_e} \beta \, d\bar{r}} + e^{-\int \beta \, d\bar{r}} \int_{\bar{r}_e}^{\bar{r}} e^{\int \beta \, d\bar{r}} (\beta - 2) \, d\bar{r} \tag{19}$$

For constant L/D and $\bar{\Phi}$, and small and slowly changing γ, β is approximately a constant, or a mean value is assumed for $\bar{\gamma}$, and Eq. (19) can be reduced to

$$V^2 = 1 - \frac{2}{\beta} - \left(1 - \frac{2}{\beta} - V_e^2\right) e^{\beta(\bar{r}_e - \bar{r})} \tag{20}$$

Equation (20) gives the relation between altitude and velocity for constant values of β. Since β is a function of flight-path angle, L/D ratio, and bank angle, any changes in one of these quantities will affect the vehicle flight-speed and altitude relationship. Dividing Eq. (16) by Eq. (15) and taking β and $\bar{\gamma}$ at mean values, respectively, one can obtain the turn angle:

$$\omega = \frac{\tan \bar{\phi}}{\bar{\gamma}(\beta - 2)} \left[\frac{2}{\beta} \ln \frac{\beta V^2 - \beta + 2}{\beta V_e^2 - \beta + 2} + \ln \frac{V_e^2}{V^2} \right] \tag{21}$$

or

$$\omega = \frac{\tan \bar{\phi}}{\bar{\gamma}(\beta - 2)} \left[2(\bar{r}_e - \bar{r}) - \ln \frac{1 - \frac{2}{\beta} - \left(1 - \frac{2}{\beta} - V_e^2\right) e^{\beta(\bar{r}_e - \bar{r})}}{V_e^2} \right] \tag{22}$$

In the flight regime of interest, γ is small and slowly changing. Therefore it is assumed that a mean value, $\bar{\gamma}$, can be obtained. The initial turn angle is taken as zero in Eqs. (21) and (22). Dividing Eq. (14) by Eq. (15), one obtains

$$\frac{1}{g} \dot{u} - \frac{1}{u_o^2 \frac{L}{D} \cos \bar{\phi}} u^2 = \gamma - \frac{1}{\frac{L}{D} \cos \bar{\phi}} \tag{23}$$

Solving Eq. (23) for t as a function of V by assuming constant L/D and $\bar{\phi}$ and mean value $\bar{\gamma}$,

$$t = \frac{u_o \frac{L}{D} \cos \bar{\phi}}{2g} \sqrt{\frac{\beta}{\beta - 2}} \ln \frac{[V\sqrt{\beta} - \sqrt{\beta - 2}][V_e\sqrt{\beta} + \sqrt{\beta - 2}]}{[V\sqrt{\beta} + \sqrt{\beta - 2}][V_e\sqrt{\beta} - \sqrt{\beta - 2}]} \tag{24}$$

Noting that

$$\dot{u} = \frac{1}{2} \frac{du^2}{dS}$$

where S is the distance along the flight path, Eq. (23) can be re-written as

$$\frac{1}{2g} \frac{du^2}{dS} - \frac{1}{u_o^2 \frac{L}{D} \cos \bar{\phi}} u^2 = \gamma - \frac{1}{\frac{L}{D} \cos \bar{\phi}} \tag{23a}$$

Solving Eq. (23a) for S as a function of V and $\bar{r}$, respectively, one obtains

$$S = \frac{R_o}{B\bar{\gamma}} \ln \frac{V^2\beta + 2 - \beta}{V_e^2\beta + 2 - \beta} \tag{25}$$

and

$$S = \frac{R_o}{\bar{\gamma}} (\bar{r}_e - \bar{r}) \tag{26}$$

where $R_o = u_o^2/g$. The downrange distance can be obtained from

$$dx = dS \cos \omega \tag{27}$$

where x is the distance traveled in the original direction of motion and can be taken as approximately the distance on earth because of the small flight-path angle and small ratio of altitude to earth radius. For constant $\bar{\rho}$ and L/D and mean value $\bar{\gamma}$, Eq. (27) can be integrated as

$$x = \frac{-R_o}{\bar{\gamma}} \int_{\bar{r}_e}^{\bar{r}} \cos\left\{\bar{\alpha}\left[2(\bar{r}_e - \bar{r}) - \ln \frac{V_e^2 + \left(1 - \frac{2}{\beta} - V_e^2\right)\left(1 - e^{\beta(\bar{r}_e - \bar{r})}\right)}{V_e^2}\right]\right\} d\bar{r} \tag{28}$$

In terms of V

$$x = \frac{R_o}{\bar{\gamma}} \int_{V_e^2}^{V^2} \frac{\cos\left\{\bar{\alpha}\left[\frac{2}{\beta} \ln \frac{\beta V^2 - \beta + 2}{\beta V_e^2 - \beta + 2} + \ln \frac{V_e^2}{V^2}\right]\right\}}{V^2\beta + 2 - \beta} dV^2 \tag{29}$$

Similarly the siderange distance can be obtained for constant $\bar{\varphi}$ and L/D and mean value $\bar{\gamma}$ from

$$dy = dS \sin \omega \tag{30}$$

where y is the distance traveled perpendicular to the original direction of motion, or

$$y = \frac{-R_o}{\bar{\gamma}} \int_{\bar{r}_e}^{\bar{r}} \sin \left\{ \bar{\alpha} \left[2(\bar{r}_e - \bar{r}) - \ell n \frac{V_e^2 + \left(1 - \frac{2}{\beta} - V_e^2\right)\left(1 - e^{\beta(\bar{r}_e - \bar{r})}\right)}{V_e^2} \right] \right\} d\bar{r} \tag{31}$$

In terms of V

$$y = \frac{R_o}{\bar{\gamma}} \int_{V_e^2}^{V^2} \frac{\sin \left\{ \bar{\alpha} \left[\frac{2}{\beta} \ell n \frac{\beta V^2 - \beta + 2}{\beta V_e^2 - \beta + 2} + \ell n \frac{V_e^2}{V^2} \right] \right\}}{V^2 \beta + 2 - \beta} dV^2 \tag{32}$$

where $\bar{\alpha} = \tan \bar{\varphi}/(\beta - 2)\bar{\gamma}$

GLIDE REENTRY TRAJECTORIES AT VERY SMALL FLIGHT-PATH ANGLE

For equilibrium glide at very small flight-path angle, such as for high-L/D flight, $\gamma \approx \dot{\gamma} \approx 0$. Equations (4) to (6) can be reduced to

$$\frac{\dot{u}}{g} = -\frac{D}{W} \tag{33}$$

$$\frac{L}{W} \cos \bar{\varphi} = 1 - \frac{u^2}{u_o^2} \tag{34}$$

$$\frac{u}{g}\dot{\omega} = \frac{L}{W}\sin\phi \tag{35}$$

From the definition of β

$$\frac{2}{\beta} = \gamma\frac{L}{D}\cos\phi = 0 \tag{36}$$

Substituting Eq. (36) into Eqs. (21), (24), (25), (29), and (32), respectively, one obtains

$$\omega = \frac{L}{D}\sin\phi\ \ell n\frac{V_i}{V} \tag{37}$$

$$t = \frac{u_o\frac{L}{D}\cos\phi}{2g}\ \ell n\frac{(V-1)(V_i+1)}{(V+1)(V_i-1)} \tag{38}$$

$$S = \frac{1}{2}R_o\frac{L}{D}\cos\phi\ \ell n\frac{1-V^2}{1+V_i^2} \tag{39}$$

$$x = \frac{1}{2}R_o\frac{L}{D}\cos\phi\int_{V_i^2}^{V^2}\frac{\cos\left[\frac{1}{2}\frac{L}{D}\sin\phi\ \ell n\frac{V_i^2}{V^2}\right]dV^2}{V^2-1} \tag{40}$$

$$y = \frac{1}{2}R_o\frac{L}{D}\cos\phi\int_{V_i^2}^{V^2}\frac{\sin\left[\frac{1}{2}\frac{L}{D}\sin\phi\ \ell n\frac{V_i^2}{V^2}\right]dV^2}{V^2-1} \tag{41}$$

where $V_i = u_i/u_o$, and u_i = initial speed.

Equations (33) and (34) and their results, Eqs. (37) to (41), are the same as obtained by Nyland.[12]

NEAR-CONSTANT-SPEED GLIDE AT HIGH ALTITUDE

For some applications of atmospheric flight, it may be desirable to have the lifting vehicle enter at near-orbital speed and fly at maximum L/D ratio or maximum C_L and at constant bank angle until it reaches denser atmosphere at an altitude of about 250,000 ft. In this phase of flight at high altitude, atmospheric drag is assumed to be nearly equal and opposite to the component of gravity along the flight path. Thus, there would be little change in vehicle speed and, in the present notation, this implies that $1/V^2 - 1 \approx 0$. Let the atmospheric density be expressed by the well-known exponential approximation or

$$\rho = \rho_o e^{-\zeta h} \tag{42}$$

where ρ_o is the reference atmospheric density and ζ is the inverse scale height. Substituting Eq. (42) into Eq. (7),

$$\bar{\rho} = \frac{\rho_o u_o^2}{W/A} e^{-\zeta h} = \frac{\rho_o u_o^2}{W/A} e^{-\bar{\zeta} r} \tag{43}$$

where $\bar{\zeta} = \zeta(R_E + h_e) \approx \zeta R_E$.

Then for flight at small angles of inclination, Eqs. (4) to (6) can be reduced to

$$\frac{\dot{u}}{g} = \gamma - \frac{D}{W} \tag{44}$$

$$-\frac{u}{g}\dot{\gamma} = \frac{L}{W}\cos\phi \tag{45}$$

$$\frac{u}{g}\dot{\omega} = \frac{L}{W}\sin\phi \tag{46}$$

Or in terms of V and $\bar{r}$, Eqs. (44) to (46) become

$$\frac{dV^2}{d\bar{r}} = \frac{1}{\gamma} \frac{\rho_o u_o^2}{W/C_D A} e^{-\bar{\zeta}\bar{r}} V^2 - 2 \tag{44a}$$

$$\frac{d\gamma^2}{d\bar{r}} = \frac{\rho_o u_o^2}{W/C_L A} e^{-\bar{\zeta}\bar{r}} \cos \phi \tag{45a}$$

$$\frac{d\omega}{d\bar{r}} = - \frac{1}{2\gamma} \frac{\rho_o u_o^2}{W/C_L A} e^{-\bar{\zeta}\bar{r}} \sin \phi \tag{46a}$$

Let

$$D_D = \frac{\rho_o u_o^2}{W/C_D A}$$

$$D_L = \frac{\rho_o u_o^2}{W/C_L A}$$

Then Eqs. (44a) to (46a) can be rewritten as

$$\frac{dV^2}{d\bar{r}} = \frac{1}{\gamma} D_D e^{-\bar{\zeta}\bar{r}} V^2 - 2 \tag{44b}$$

$$\frac{d\gamma^2}{d\bar{r}} = D_L e^{-\bar{\zeta}\bar{r}} \cos \phi \tag{45b}$$

$$\frac{d\omega}{d\bar{r}} = - \frac{1}{2\gamma} D_L e^{-\zeta r} \sin \phi \tag{46b}$$

For constant $W/C_L A$, Eq. (45a) can be readily integrated to yield

$$\gamma^2 = \gamma_e^2 + D_L \frac{\cos \Phi}{\bar{\zeta}} \left[e^{-\bar{\zeta}\bar{r}_e} - e^{-\bar{\zeta}\bar{r}} \right] = A_1 - B_1 e^{-\bar{\zeta}\bar{r}} \qquad (47)$$

where

γ_e = flight-path angle at entry

$\bar{r}_e$ = dimensionless altitude at entry

$$A_1 = \gamma_e^2 + B_1 e^{-\bar{\zeta}\bar{r}_e}$$

$$B_1 = D_L(\cos \Phi/\bar{\zeta})$$

Hence

$$\gamma = \left(A_1 - B_1 e^{-\bar{\zeta}\bar{r}} \right)^{\frac{1}{2}}$$

$$\frac{1}{\gamma} = \frac{1}{\sqrt{A_1}\left(1 - \frac{B_1}{A_1} e^{-\bar{\zeta}\bar{r}} \right)^{\frac{1}{2}}}$$

$$= \frac{1}{\sqrt{A_1}} \left[1 - \frac{1}{2} \frac{B_1}{A_1} e^{-\bar{\zeta}\bar{r}} + \ldots \right]$$

But

$$\frac{B_1}{A_1} e^{-\bar{\zeta}\bar{r}} \ll 1$$

$$\therefore \frac{1}{\gamma} \approx \frac{1}{\sqrt{A_1}} = \left(\gamma_e^2 + B_1 e^{-\bar{\zeta}\bar{r}_e} \right)^{-\frac{1}{2}} \approx \frac{1}{\gamma_e} \qquad (48)$$

Substituting Eq. (48) into Eqs. (44a) and (46a), respectively,

$$\frac{dV^2}{d\bar{r}} - \frac{1}{\sqrt{A_1}} D_D e^{-\bar{\zeta}\bar{r}} V^2 = -2 \qquad (49)$$

$$\frac{d\omega}{d\bar{r}} + \frac{1}{2\sqrt{A_1}} D_L e^{-\bar{\zeta}\bar{r}} \sin \Phi = 0 \tag{50}$$

Integrating Eqs. (49) and (50) for constant $W/C_D A$,

$$V^2 = V_e^2 e^{\frac{D_D}{\sqrt{A_1}} \frac{1}{\bar{\zeta}} \left(e^{-\bar{\zeta}\bar{r}_e} - e^{-\bar{\zeta}\bar{r}} \right)} - \frac{D}{\sqrt{A_1}} \frac{1}{\bar{\zeta}} e^{-\bar{\zeta}\bar{r}} + 2e^{\int_{\bar{r}}^{\bar{r}_e} \frac{D_D}{\sqrt{A_1}} \frac{1}{\bar{\zeta}} e^{-\bar{\zeta}\bar{r}} \, d\bar{r}} \tag{51}$$

$$\omega = \frac{D_L}{2\sqrt{A_1}\,\bar{\zeta}} \sin \Phi \left[e^{-\bar{\zeta}\bar{r}} - e^{-\bar{\zeta}\bar{r}_e} \right] + \omega_e \tag{52}$$

where V_e and ω_e are initial values of reentry velocity ratio and reentry turn angle, respectively.

CONSTANT-DECELERATION GLIDE AT CONSTANT ALTITUDE

After rapid and close to constant velocity descent from orbit to an altitude of about 250,000 ft, many entries of interest may require the vehicle to fly at constant altitude to perform plane-change maneuvers. In order to maintain vehicle glide at constant altitude, the gravity has to be balanced by lift force. As the vehicle decelerates, the lift coefficient has to increase to overcome the reduction in dynamic pressure until the lift force is too small to sustain constant-altitude flight. In this phase of flight h is essentially constant and $\gamma = \dot{\gamma} = 0$. The governing equations of motion are identical to that for equilibrium glide at very small flight-path angle except that L and D are variables, namely,

$$\frac{\dot{u}}{g} = -\frac{D}{W} \tag{53}$$

$$\frac{L}{W}\cos\Phi = 1 - \frac{u^2}{u_o^2} \tag{54}$$

$$\frac{u}{g}\dot{\omega} = \frac{L}{W}\sin\Phi \tag{55}$$

However, in order to prevent skip, the vehicle is required to fly at variable L/D at almost constant altitude. In addition, the vehicle may fly at certain fixed bank angles to achieve desired plane changes. For manned maneuverable vehicles, it may be desirable to perform this aerodynamic maneuvering in a constant-deceleration mode of flight. Then $\dot{u}$ and D become constants. Therefore, it is assumed that the L/D ratio follows the relationship suggested by Cohen,[10] namely,

$$\frac{C_L}{C_D} = A_2\left(1 - \frac{u^2}{u_o^2}\right) = \frac{L}{D} \tag{56}$$

Substituting Eq. (56) into Eq. (54),

$$D = \frac{W}{A_2\cos\Phi} \tag{57}$$

or

$$C_D = \frac{2}{V^2 A_2 \bar{\rho}\cos\Phi} \tag{58}$$

where $A_2 = -1/\dot{u}/g\cos\Phi$ is constant and deceleration ($-\dot{u}$) can be specified in g's. Equation (56) can also be rewritten as

$$C_L = \frac{2A_2}{\bar{\rho}\cos\Phi}\left(\frac{1 - V^2}{V^2}\right) \tag{59}$$

Then Eq. (53) can be rewritten as

$$\dot{V} = \frac{\dot{u}}{u_o} = \text{constant}$$

Therefore flight is at a constant rate of deceleration, and

$$V = V_i + \frac{\dot{u}}{u_o} t \tag{60}$$

Solving Eq. (55), one obtains

$$\omega = \omega_i + \frac{g \tan \Phi}{u_o} \left[\frac{u_o}{\dot{u}} \ln V + \frac{t}{2} (V_i + V) \right] \tag{61}$$

or

$$\omega = \omega_i - \frac{g}{2\dot{u}} \tan \Phi \left(\ln \frac{V_i^2}{V^2} + V^2 - V_i^2 \right) \tag{62}$$

For a bank angle $\Phi \to 90$ deg, Eqs. (61) and (62) approach infinity and the results are not applicable, since equations of motion are for $\Phi < 90$ deg. The vehicle range can also be obtained from Eq. (53):

$$S = \frac{u_o^2}{2\dot{u}} (V_i^2 - V^2) \tag{63}$$

CONSTANT-DECELERATION GLIDE AT FIXED FLIGHT-PATH ANGLE

For manned reentry flight, it may be desirable to maintain constant deceleration during the high-speed portion of flight after constant-altitude glide. If the flight-path angle is fixed, then Eqs. (1) to (3) can be rewritten as

$$\frac{\dot{u}}{g} = \sin \gamma - \frac{D}{W} = \text{constant} \tag{64}$$

$$0 = \frac{L}{W} \cos \Phi - \left(1 - \frac{u^2}{u_o^2}\right) \cos \gamma \tag{65}$$

$$\frac{u}{g} \dot{\omega} \cos \gamma = \frac{L}{W} \sin \Phi \tag{66}$$

Equations (64) to (66) can be rewritten in terms of new variables V and $\bar{r}$ as

$$\frac{dV^2}{d\bar{r}} = \frac{C_D \bar{\rho}}{\gamma} V^2 - \frac{2 \sin \gamma}{\gamma} \tag{64a}$$

$$0 = \frac{1}{2} C_L \bar{\rho} V^2 \frac{\cos \Phi}{\cos \gamma} - 1 - V^2 \tag{65a}$$

$$\frac{d\omega}{d\bar{r}} = - \frac{C_L \bar{\rho}}{2\gamma} \frac{\sin \Phi}{\cos \gamma} \tag{66a}$$

If the same L/D ratio expression suggested by Cohen[10] is assumed, namely,

$$\frac{C_L}{C_D} = A_2 \left(1 - \frac{u^2}{u_o^2}\right) = \frac{L}{D} \tag{56}$$

substituting Eq. (56) into Eq. (65) gives

$$D = \frac{W \cos \gamma}{A_2 \cos \Phi} \tag{67}$$

or

$$C_D = \frac{2 \cos \gamma}{V^2 A_2 \bar{\rho} \cos \Phi} \tag{68}$$

$$A_2 = \frac{-\cos \gamma}{\left(\frac{\dot{u}}{g} - \sin \gamma\right) \cos \Phi} = \text{constant}$$

Equation (66) can also be rewritten as

$$C_L = \frac{2A_2 \cos \gamma}{\bar{\rho} \cos \Phi}\left(\frac{1 - V^2}{V^2}\right) = \frac{-2 \cos^2 \gamma}{\bar{\rho}\left(\frac{\dot{u}}{g} - \sin \gamma\right) \cos^2 \Phi}\left(\frac{1 - V^2}{V^2}\right) \qquad (69)$$

Substituting Eq. (67) into Eq. (64) and integrating with respect to t,

$$V = V_i + \frac{\dot{u}}{u_o} t \qquad (70)$$

Solving Eq. (64a) for V as a function of $\bar{r}$ gives

$$V^2 = \frac{2 \sin \gamma}{\gamma} e^{\int \frac{\rho_o u_o^2}{\gamma} \frac{C_D A}{W} e^{-\bar{\zeta}\bar{r}} d\bar{r}} \int_{\bar{r}}^{\bar{r}_i} e^{-\int \frac{\rho_o u_o^2}{\gamma} \frac{C_D A}{W} e^{-\bar{\zeta}\bar{r}}} d\bar{r}$$

$$+ V_i^2 e^{\int_{\bar{r}_i}^{\bar{r}} \frac{\rho_o u_o^2}{\gamma} \frac{C_D A}{W} e^{-\bar{\zeta}\bar{r}} d\bar{r}} \qquad (71)$$

Dividing Eq. (64) by Eq. (66), one obtains

$$\omega = \omega_i + \frac{\sin \Phi}{2} \frac{g}{\dot{u}} \left[\ell n \frac{V^2}{V_i^2} + V_i^2 - V^2 \right] \qquad (72)$$

Equation (64) can be rewritten as

$$\frac{dV^2}{dS} = \frac{2\mu}{u_o^2}\left(\sin\gamma - \frac{\cos\gamma}{A_2\cos\xi}\right) \tag{64b}$$

or

$$S = S_i + \frac{u_o^2}{2\dot{u}}(V^2 - V_i^2) \tag{73}$$

III. DISCUSSION AND CONCLUSIONS

The general closed-form solutions presented in Eqs. (11) through (13) can be solved numerically if the quantities W/C_DA, W/C_LA, ρ, and Φ, as functions of altitude, are known. For special cases, such as equilibrium-glide trajectories with small and slowly changing flight-path angles, the closed-form solutions for constant L/D ratio and bank angle are given in Eqs. (20) through (22), (24) through (26), (28), (29), (31), and (32) in terms of the parameter $\beta = 2/[\gamma(L/D)\cos\Phi]$. One can directly obtain the value of β for various combinations of γ, L/D, and $\cos\Phi$ from Fig. 2. When γ and Φ are fixed, β decreases with increasing L/D. (The range of β which is of interest varies with L/D as shown in Fig. 9.)

All the results shown in Figs. 3 to 9 are for equilibrium glide, where the γ term is retained in the equations of motion and is taken at mean value. For conditions where L/D, γ, and Φ are not constants, one can divide the flight path into intervals and can apply all the results by using mean values of L/D, γ, and Φ in each interval. Total flight time and total range can be obtained by summing up all the intervals.

The flight-speed to entry-speed ratios, as functions of altitude ratios for different values of β as given by Eq. (20), are presented in Fig. 3. For a given β value, the speed ratio is fixed for a given altitude. The results also indicate that the flight speed decreases with decreasing altitude. However, the rate of decrease is slower for the higher values of β. For given values of L/D, V_e, and small and slowly changing γ, the trajectory becomes steeper with increasing bank angle. A high-L/D vehicle will, in general, fly a steeper equilibrium-glide path.

Figure 4 shows the influence of entry speed, bank angle, and flight-path angle on turn angle as expressed by Eq. (21). The result indicates that the turning rate increases as the vehicle slows down. Large turn angles can be accomplished with high L/D and steep bank angle. The effects of entry speed on turn angle are insignificant at low values of flight speed and small values of $\gamma(L/D)\sin\Phi$.

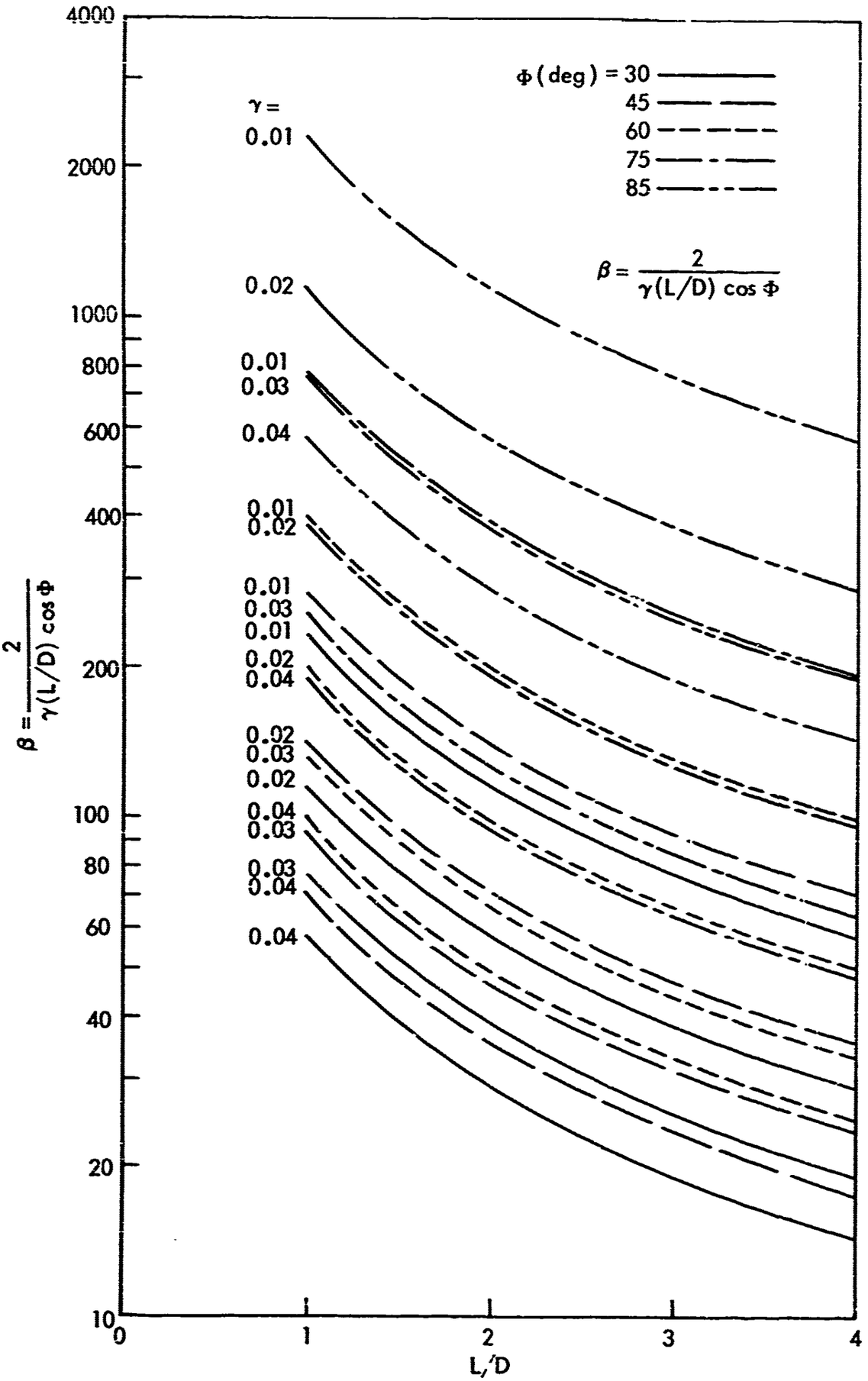

Fig. 2—Relation between flight-path angle, L/D ratio, bank angle, and parameter β

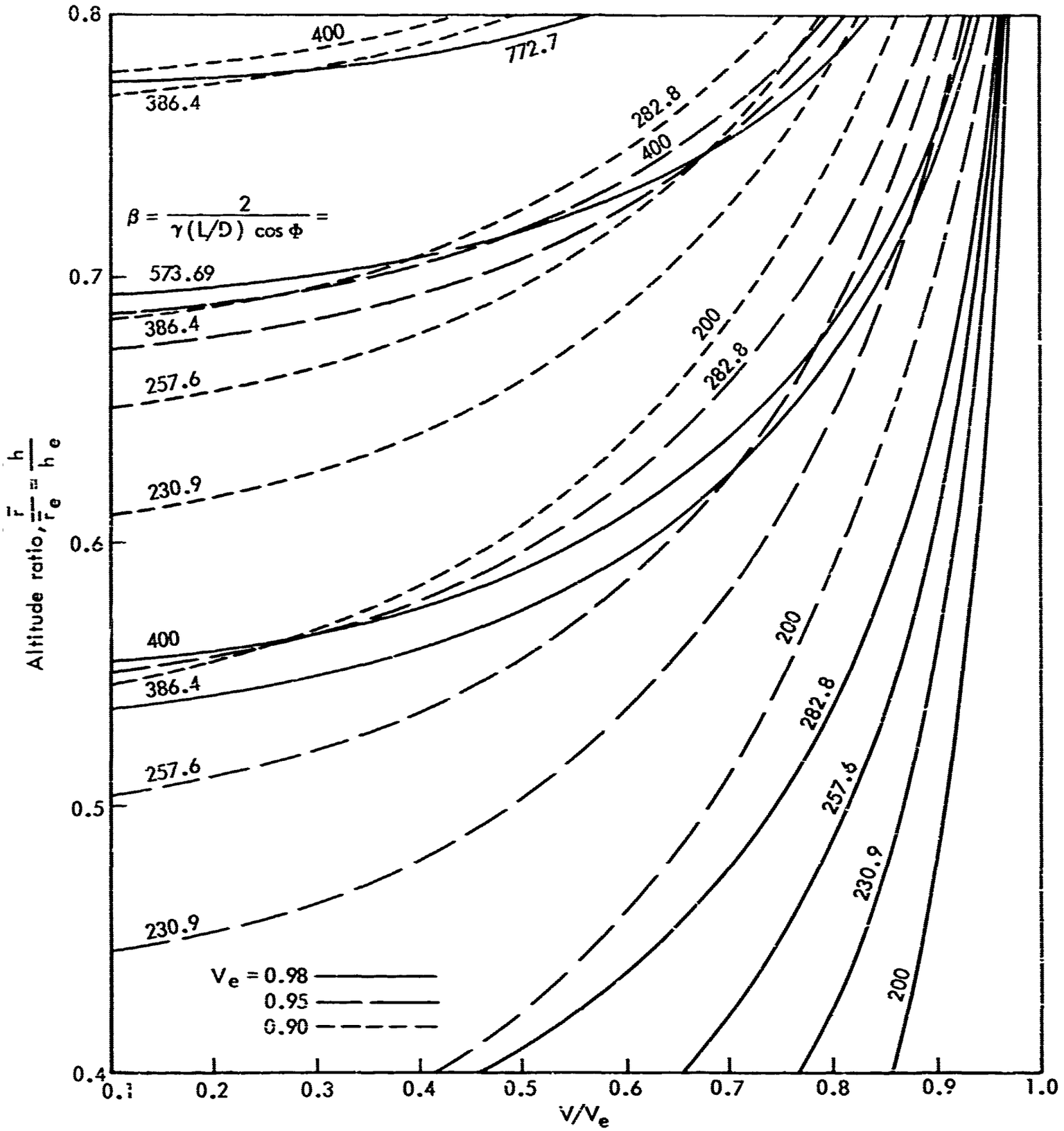

Fig. 3—Reentry glide path for constant β (Eq. (20))

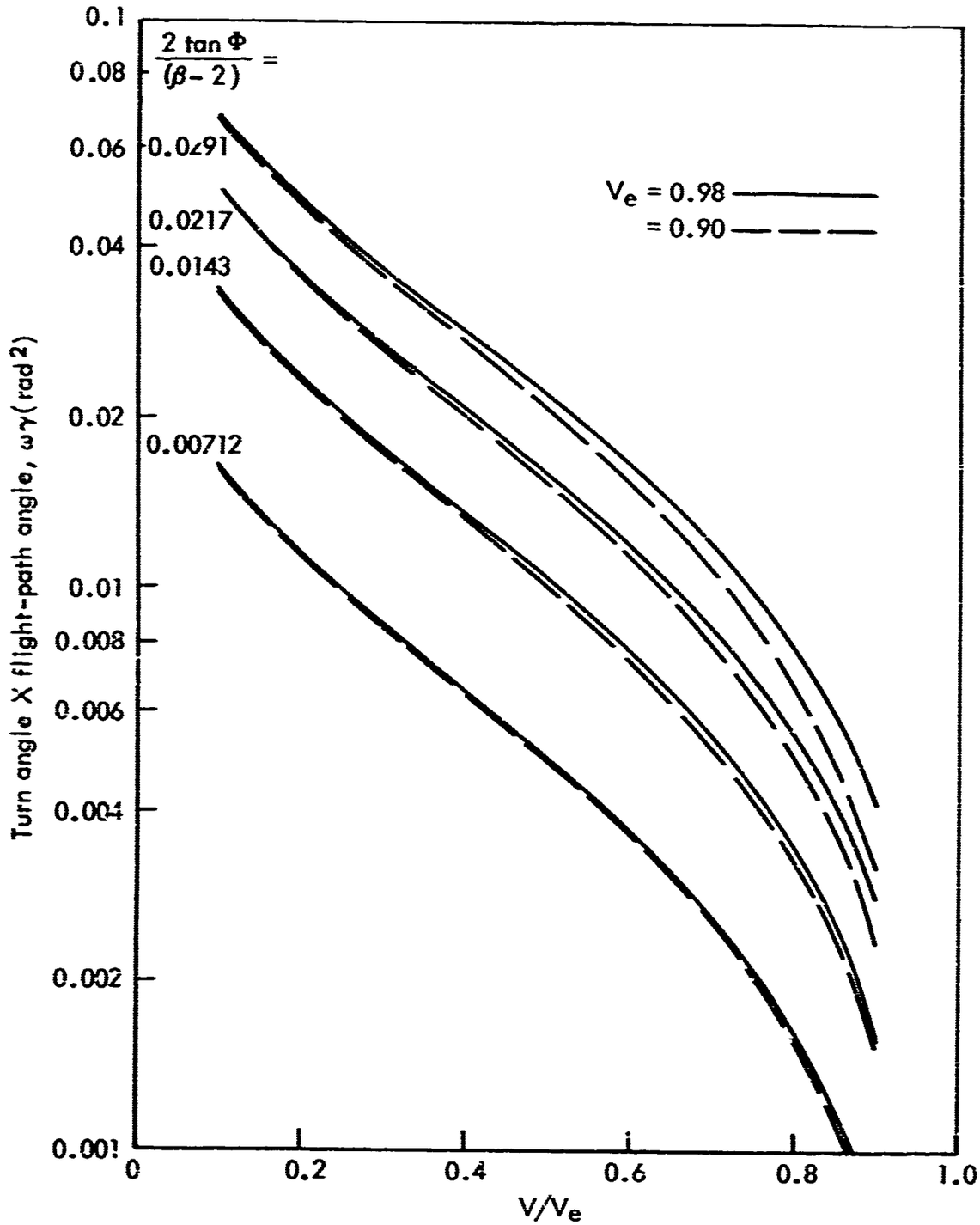

Fig. 4—Influence of entry speed, bank angle, and flight-path angle on turn angle (Eq. (21))

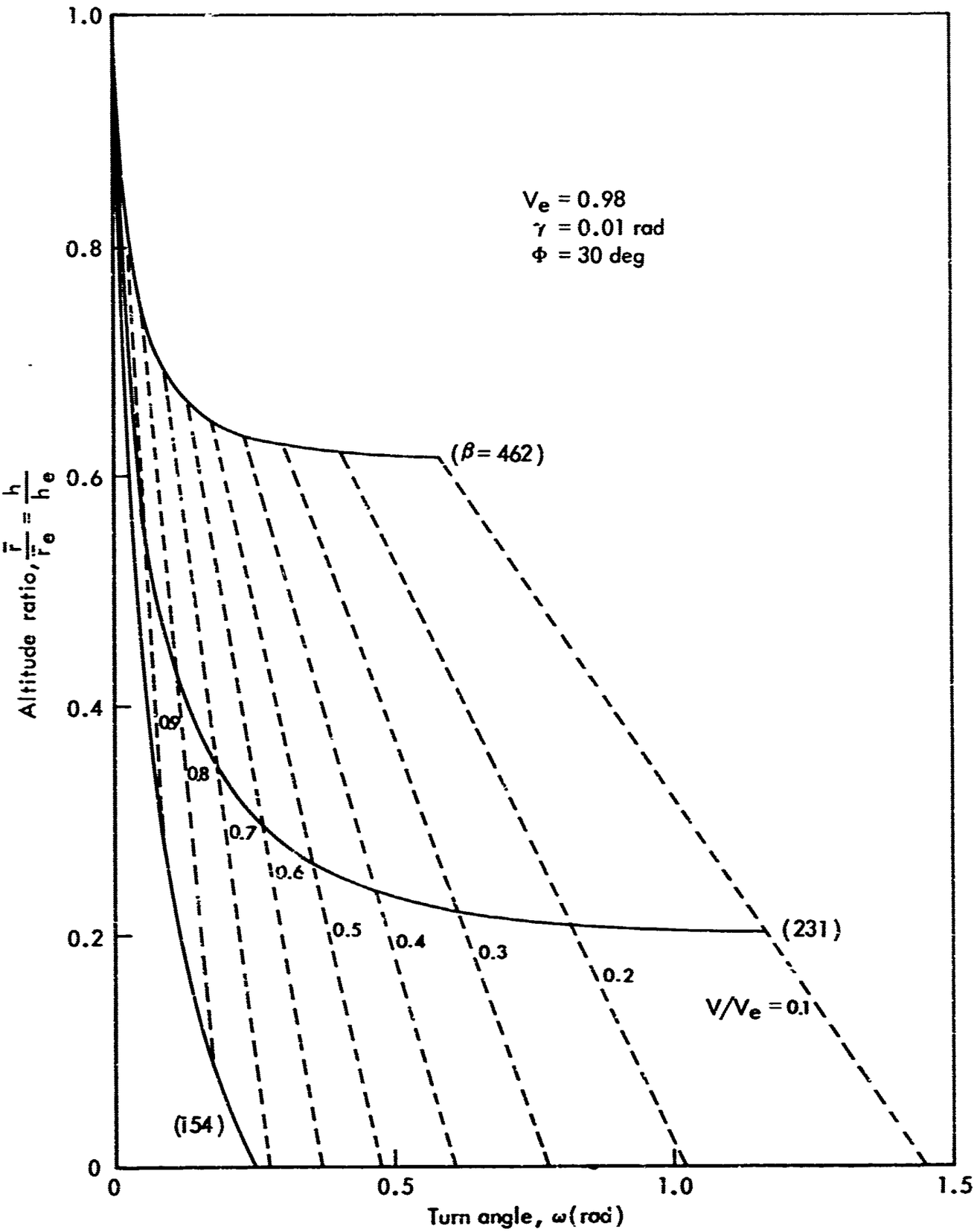

Fig.5a—Turn angle and altitude relation
($V_e = 0.98$, $\gamma = 0.01$ rad, $\Phi = 30$ deg)
(Eq. (22))

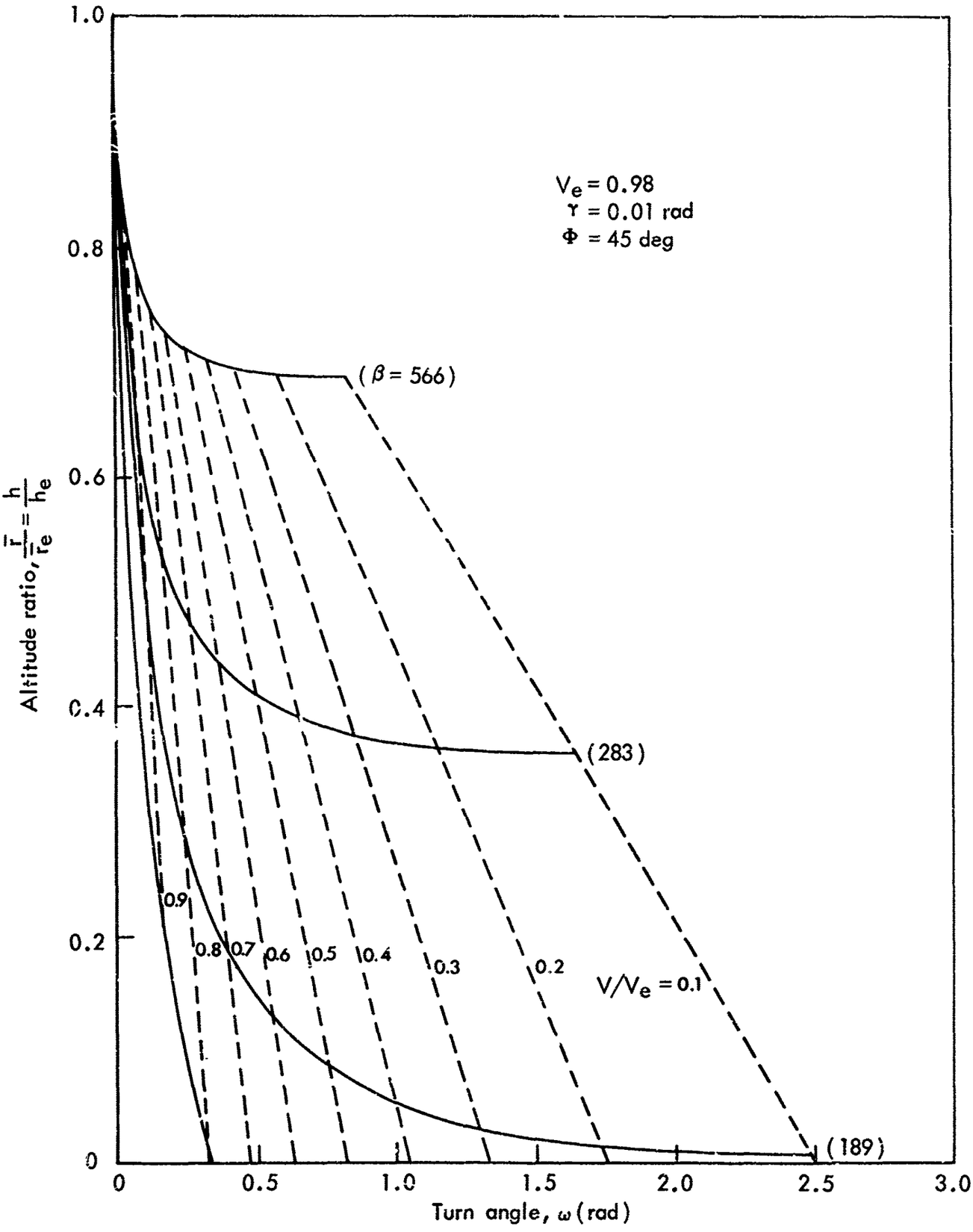

Fig.5b—Turn angle and altitude relation
($V_e = 0.98$, $\gamma = 0.01$ rad, $\Phi = 45$ deg)
(Eq. (22))

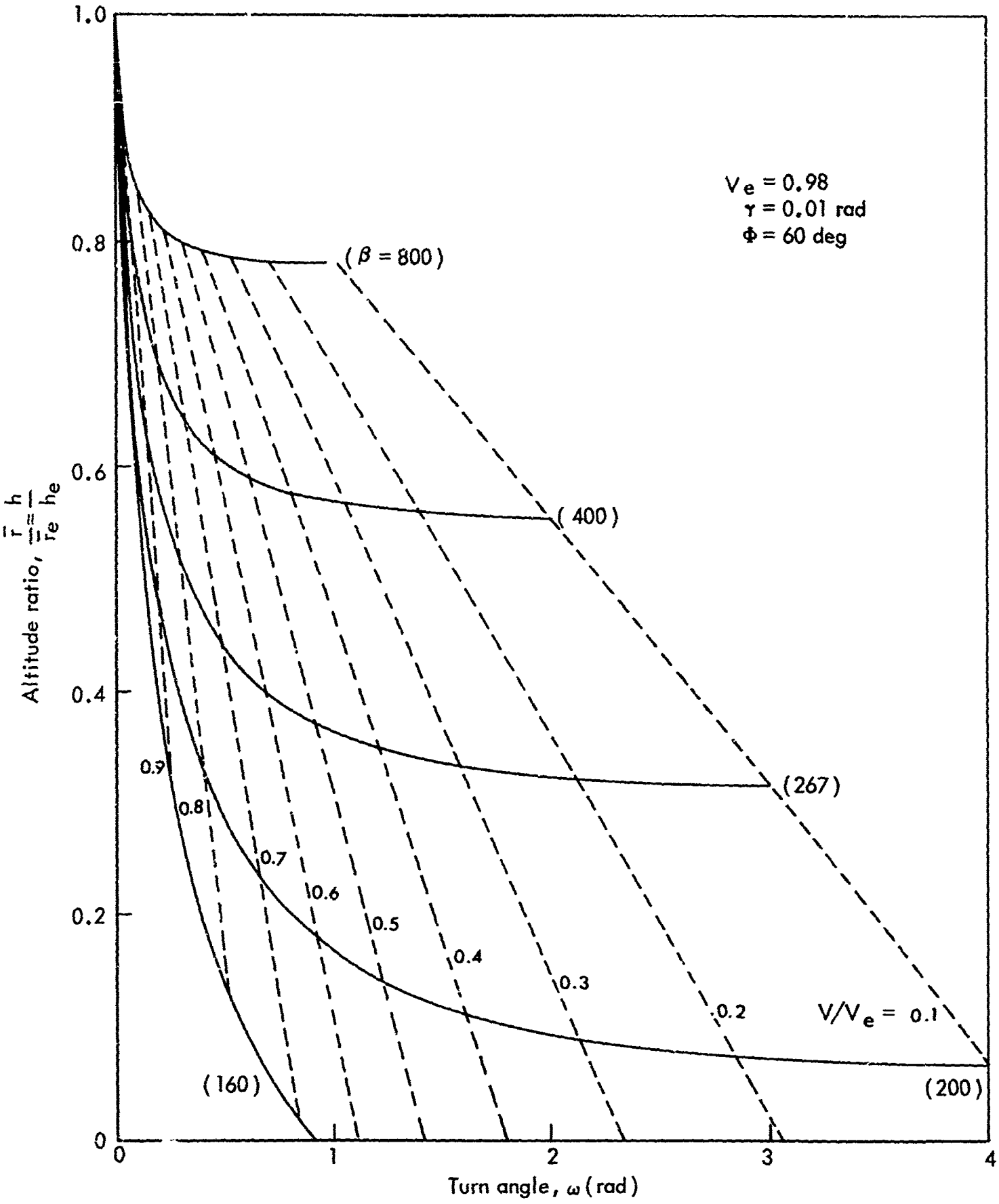

Fig.5c—Turn angle and altitude relation
($V_e = 0.98$, $\gamma = 0.01$ rad, $\Phi = 60$ deg)
(Eq. (22))

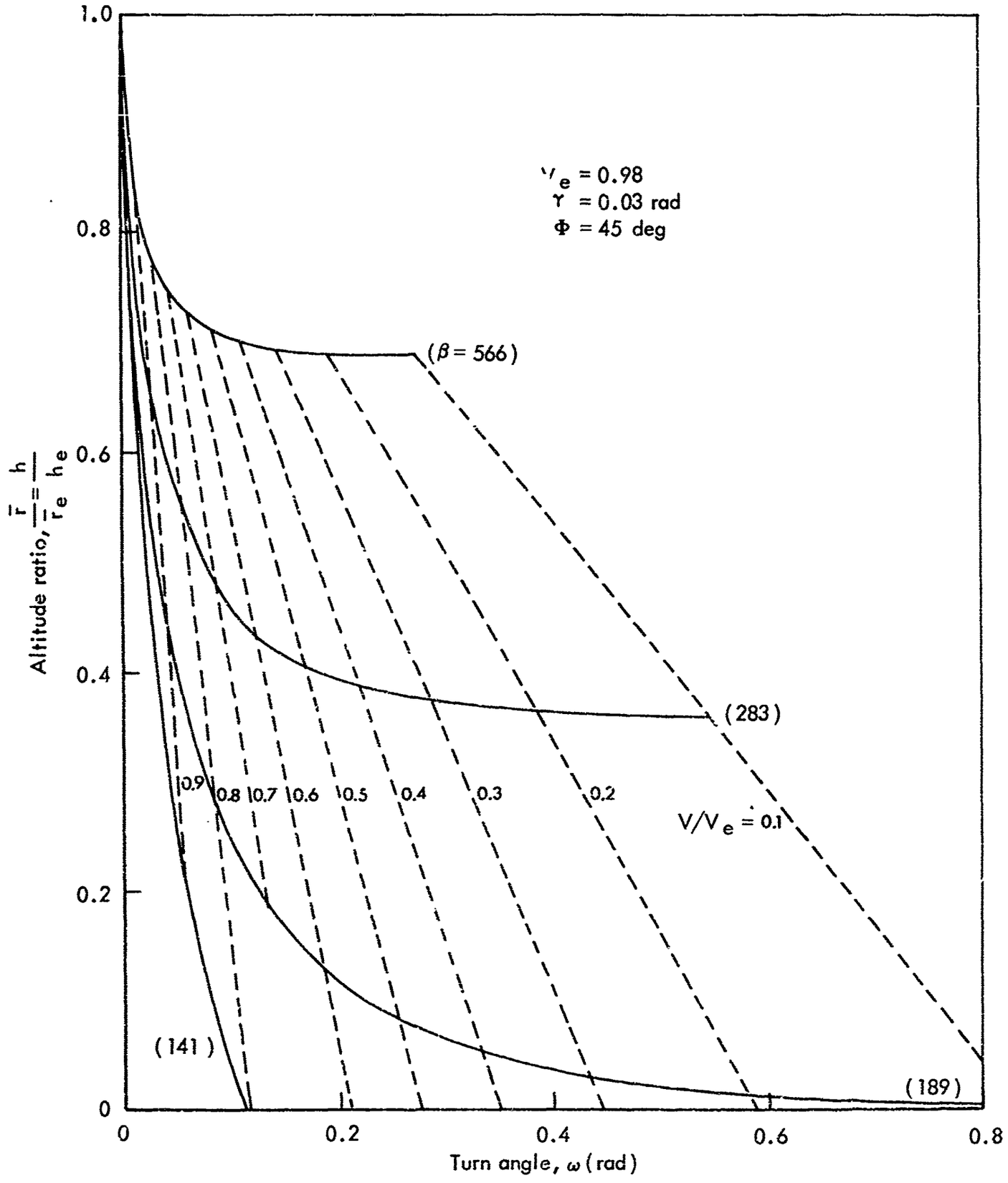

Fig. 5d—Turn angle and altitude relation
(V_e = 0.98, γ = 0.03 rad, Φ = 45 deg)
(Eq. (22))

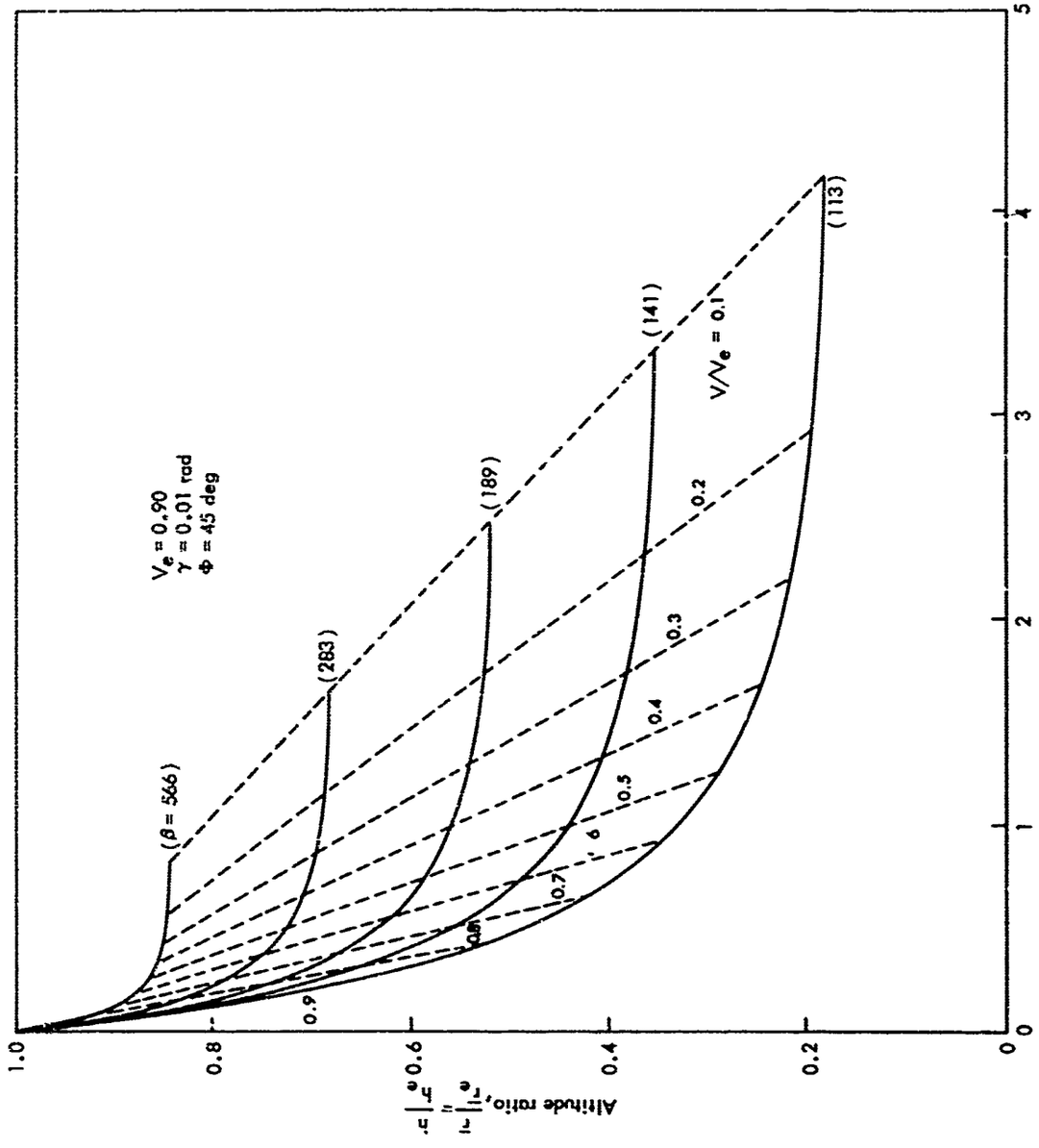

Fig. 5e—Turn angle and altitude relation
($V_e = 0.90$, $\gamma = 0.01$ rad, $\Phi = 45$ deg)
(Eq. (22))

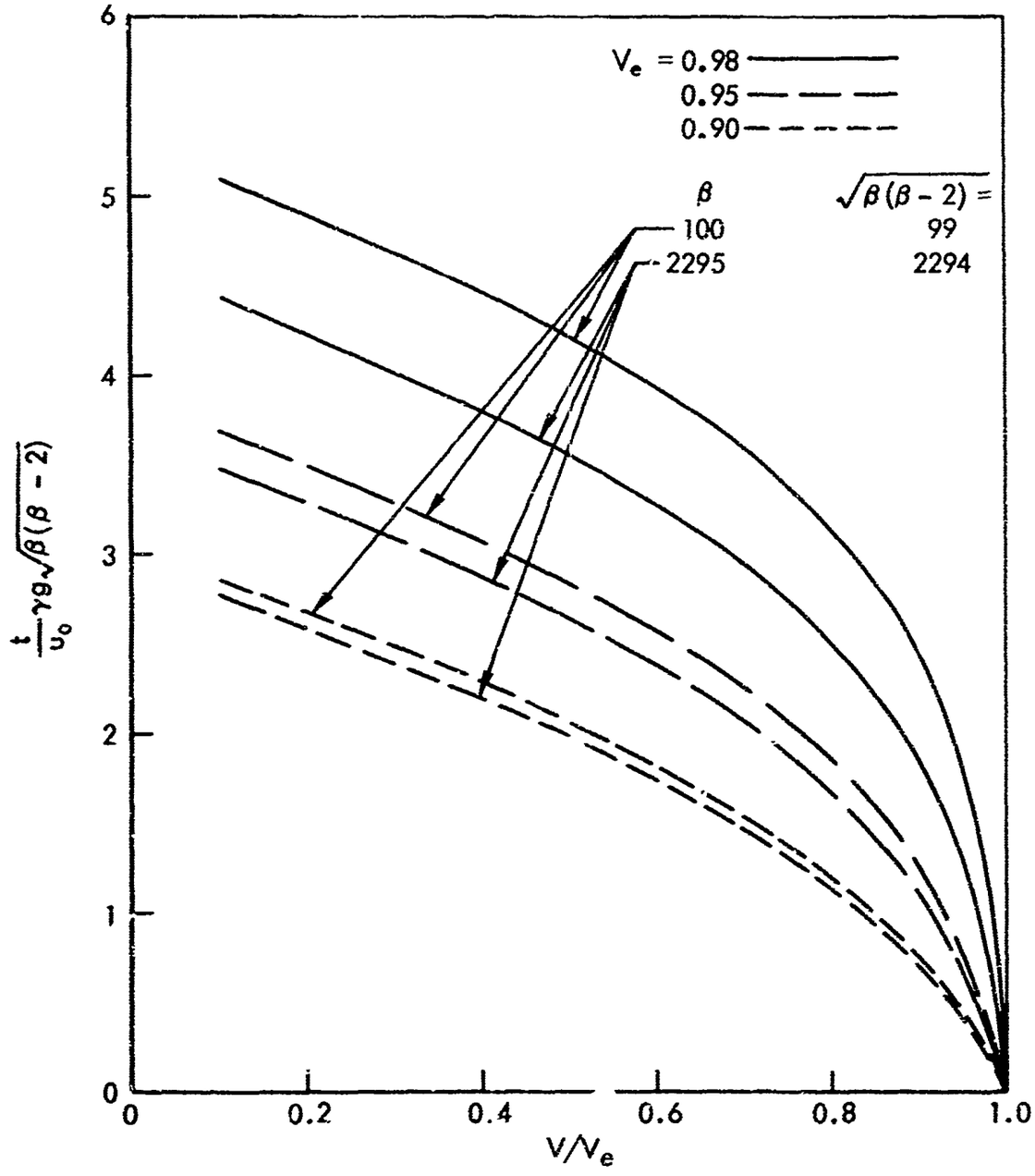

Fig. 6—Time of flight and velocity relation (Eq. (24))

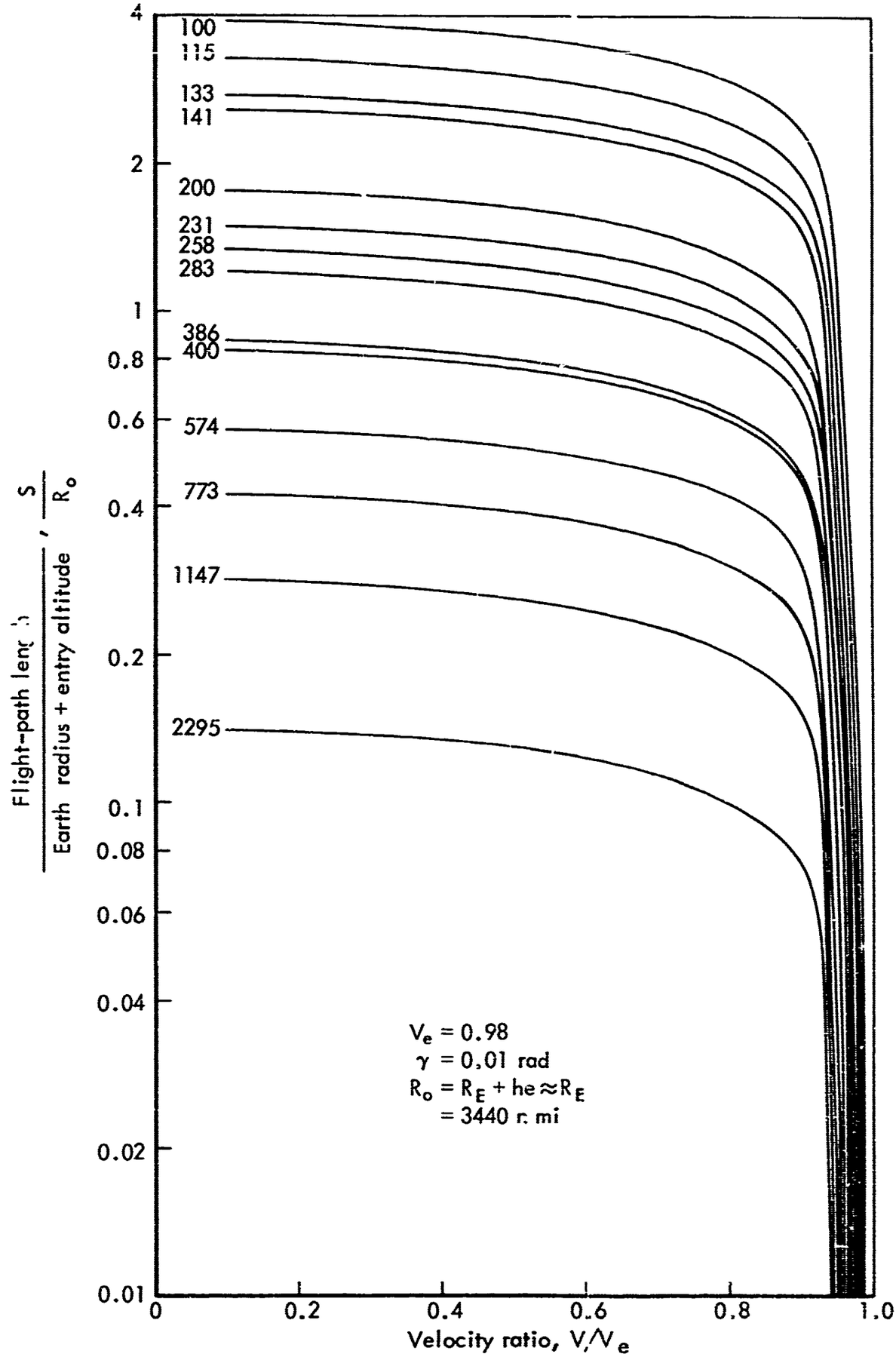

Fig. 7a—Velocity and flight-path-length relation ($\gamma = 0.01$ rad) (Eq. (25))

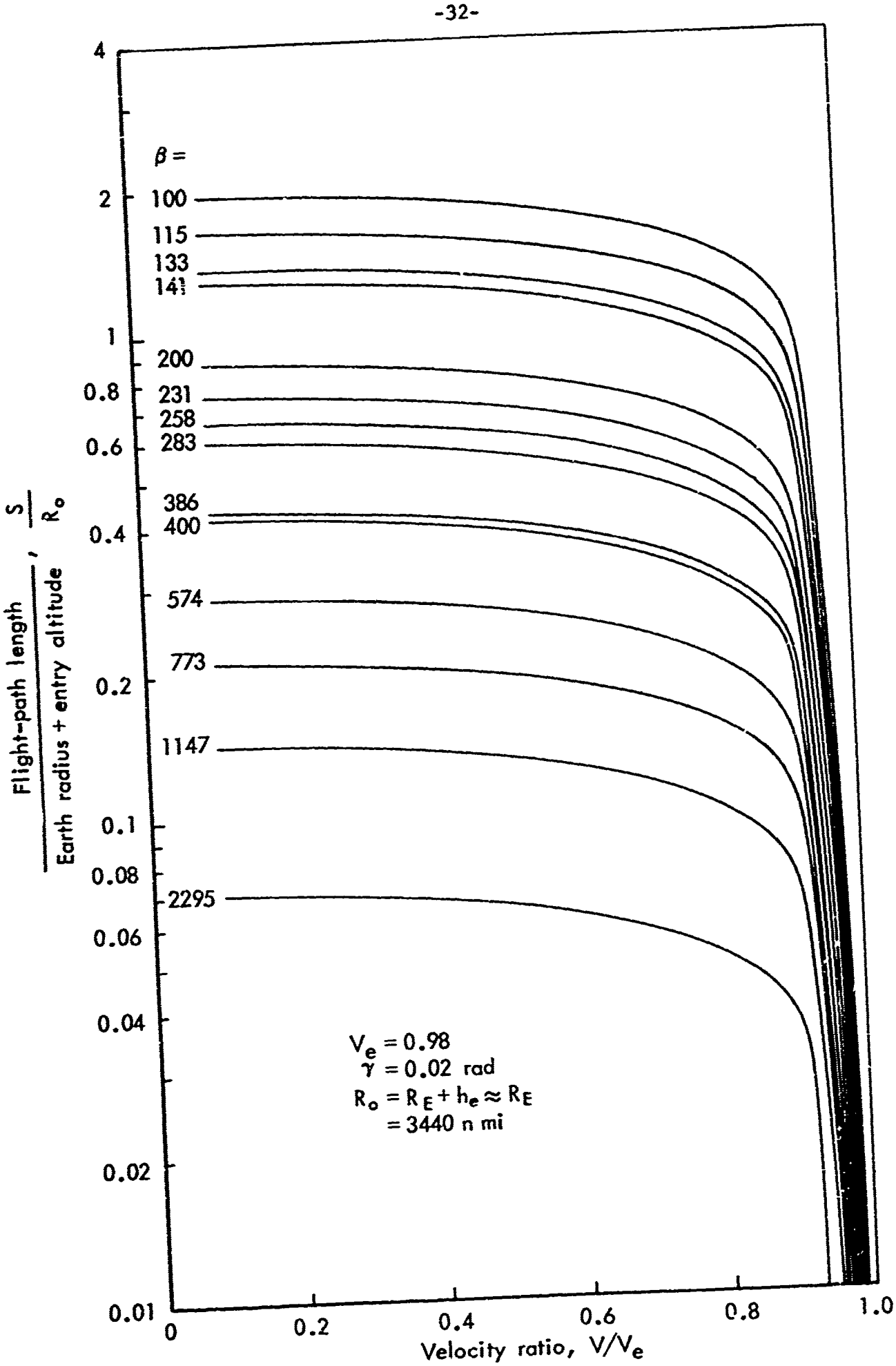

Fig. 7b—Velocity and flight-path-length relation ($\gamma = 0.02$ rad) (Eq. (25))

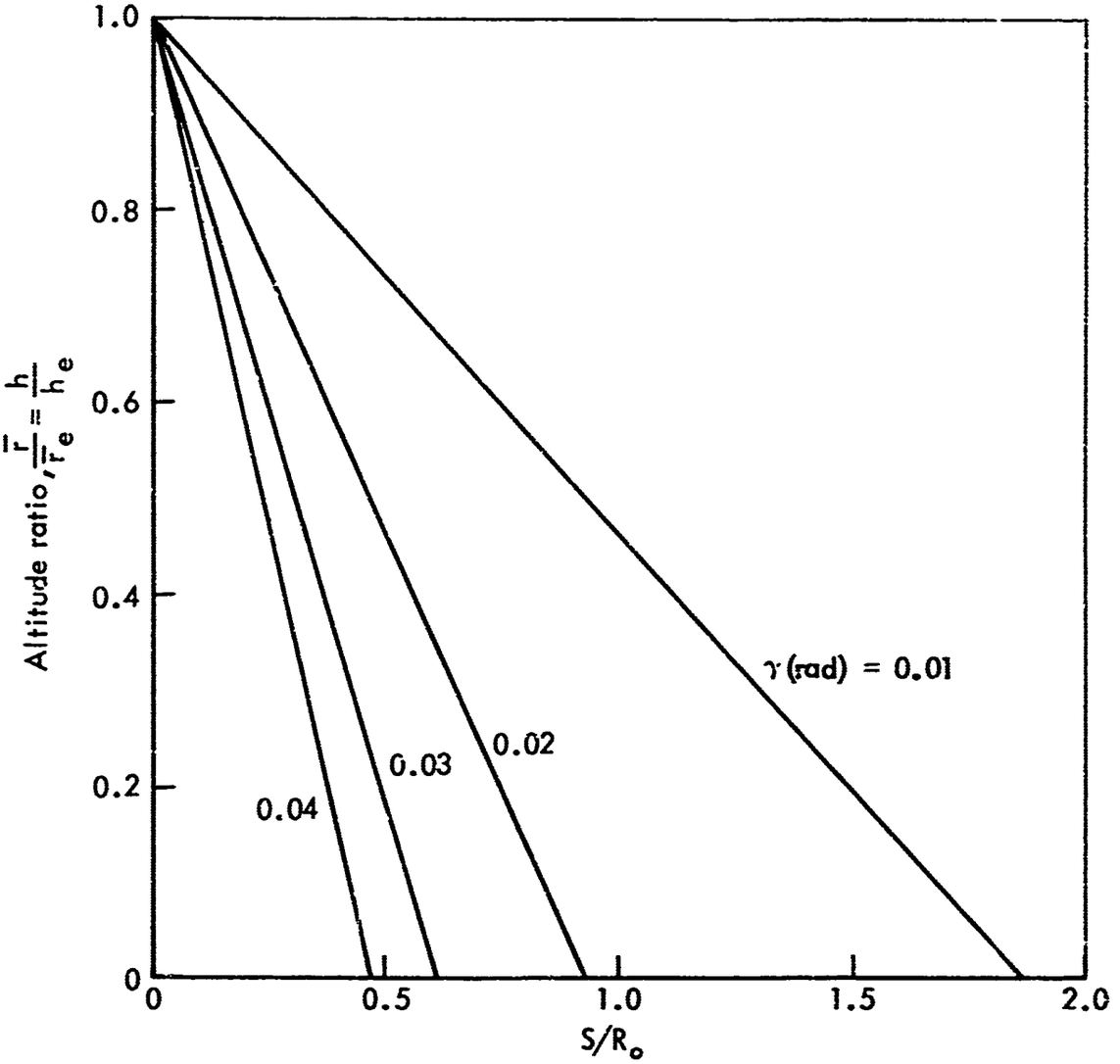

Fig.8—Flight-path length and altitude relation for constant flight-path angle (Eq. (26))

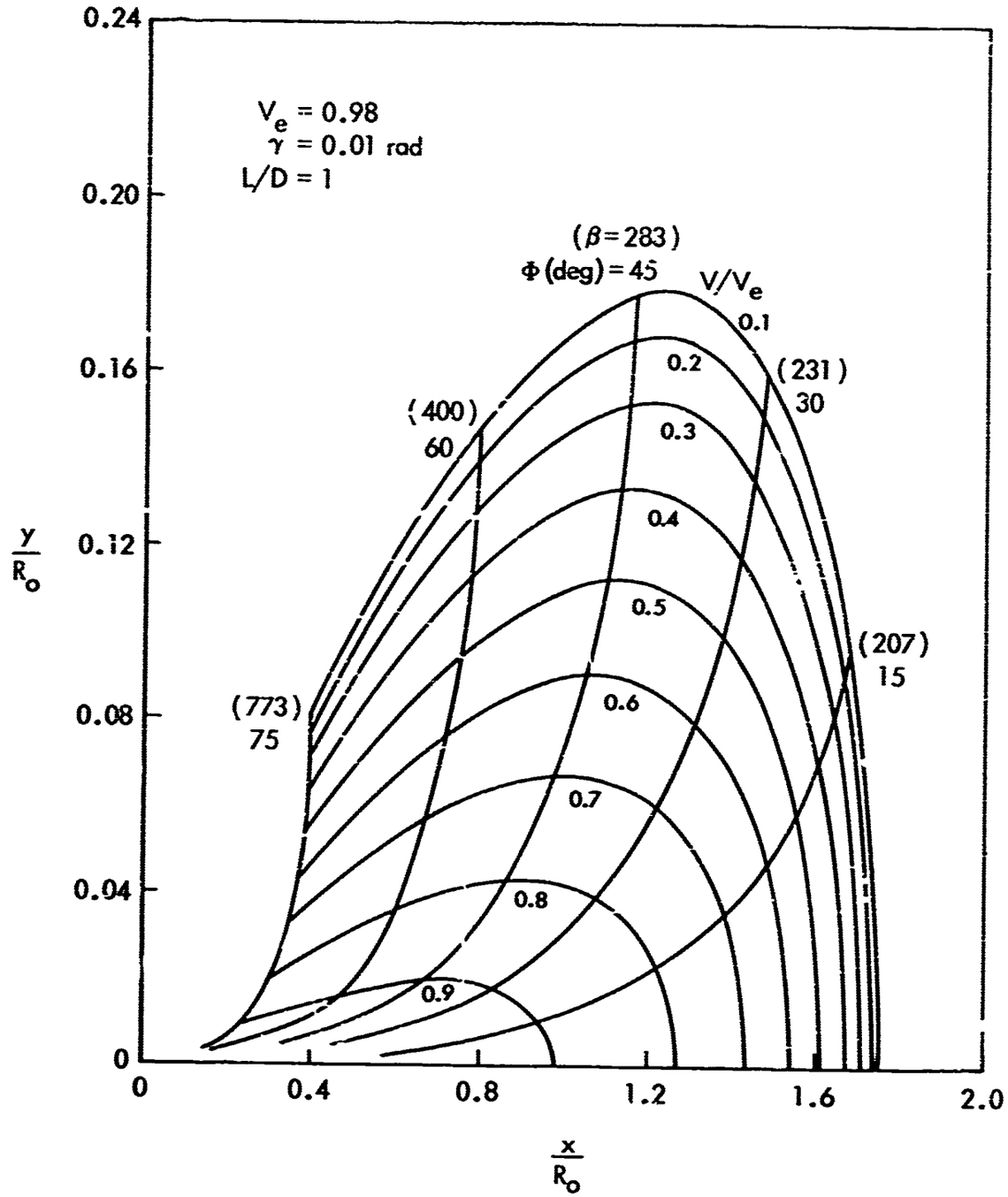

Fig. 9a—Influence of bank angle on ground trace
(L/D = 1, V_e = 0.98)
(Eqs. (29), (32))

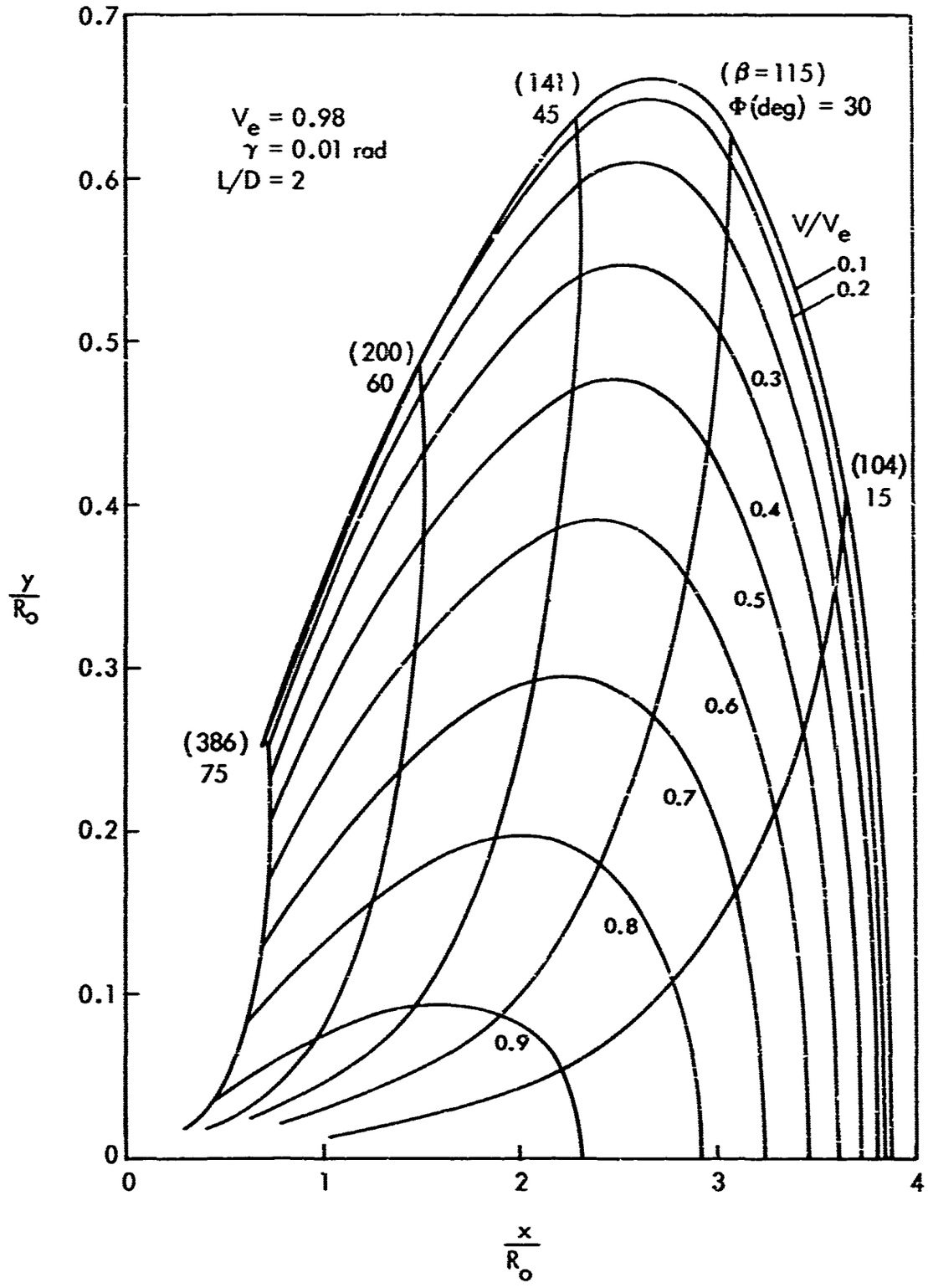

Fig. 9b—Influence of bank angle on ground trace
(L/D = 2, V_e = 0.98)
(Eqs (29), (32))

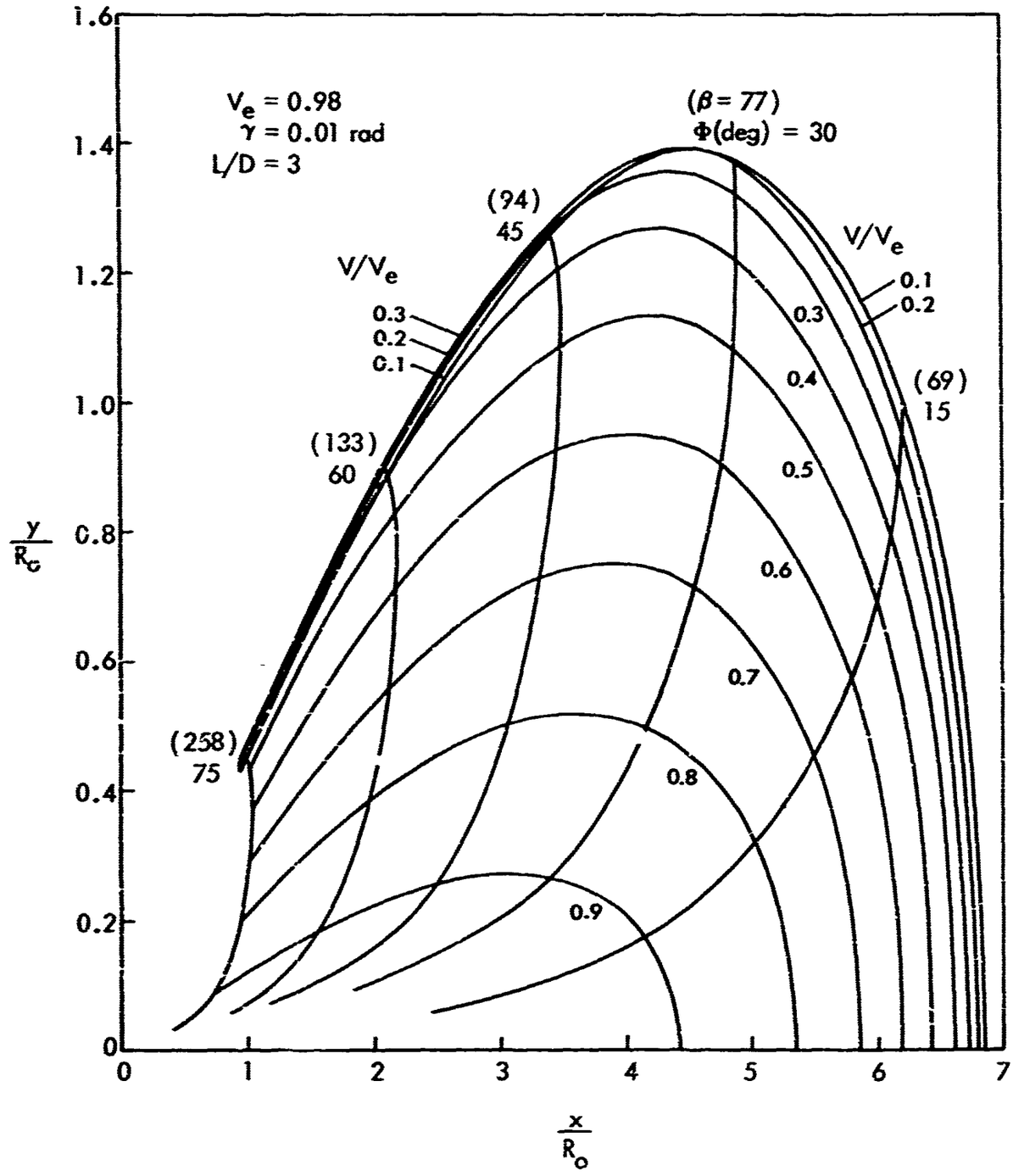

Fig. 9c—Influence of bank angle on ground trace
(L/D = 3, V_e = 0.98)
(Eqs. (29), (32))

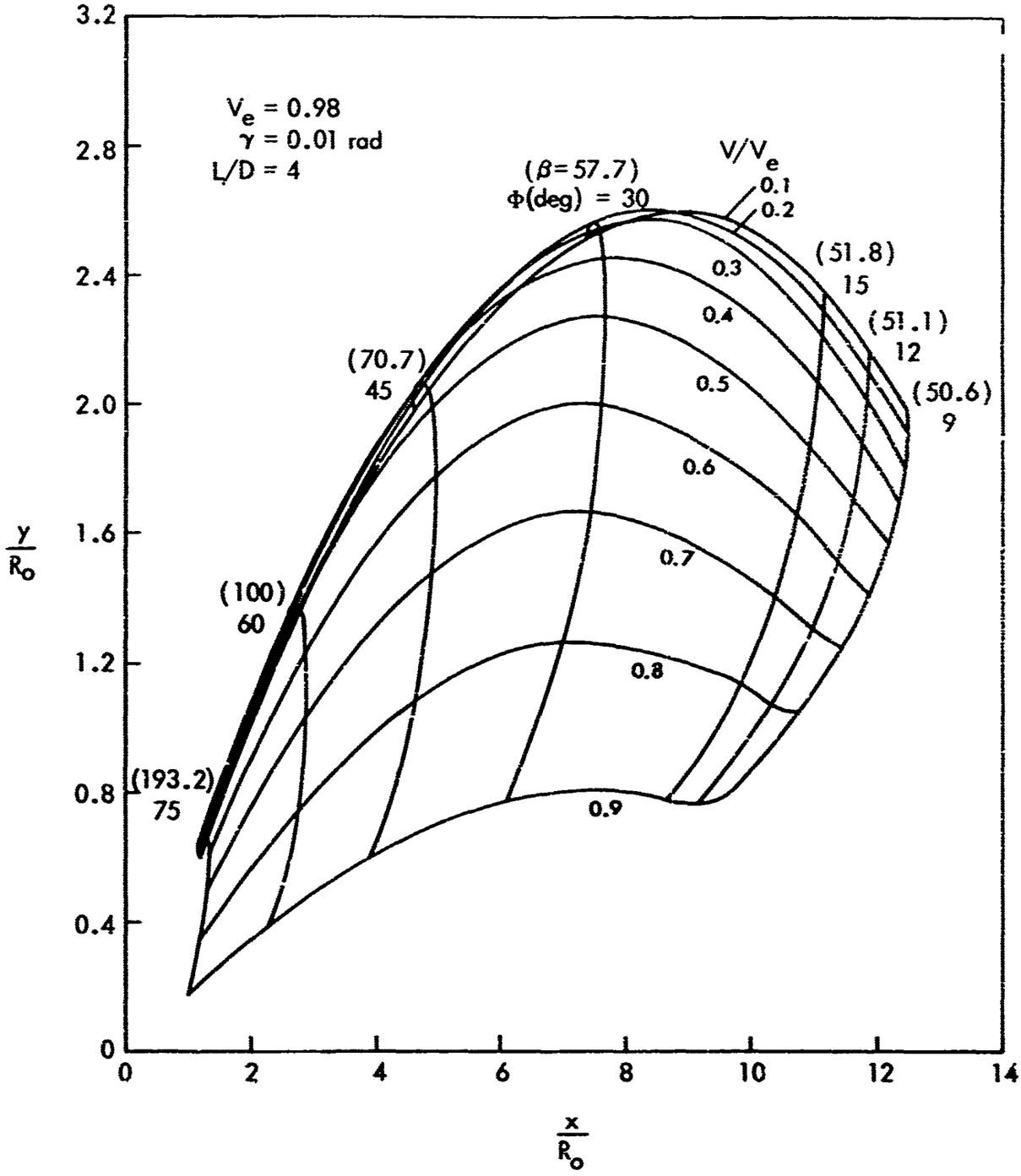

Fig. 9d—Influence of bank angle on ground trace
(L/D = 4, V_e = 0.98)
(Eqs. (29), (32))

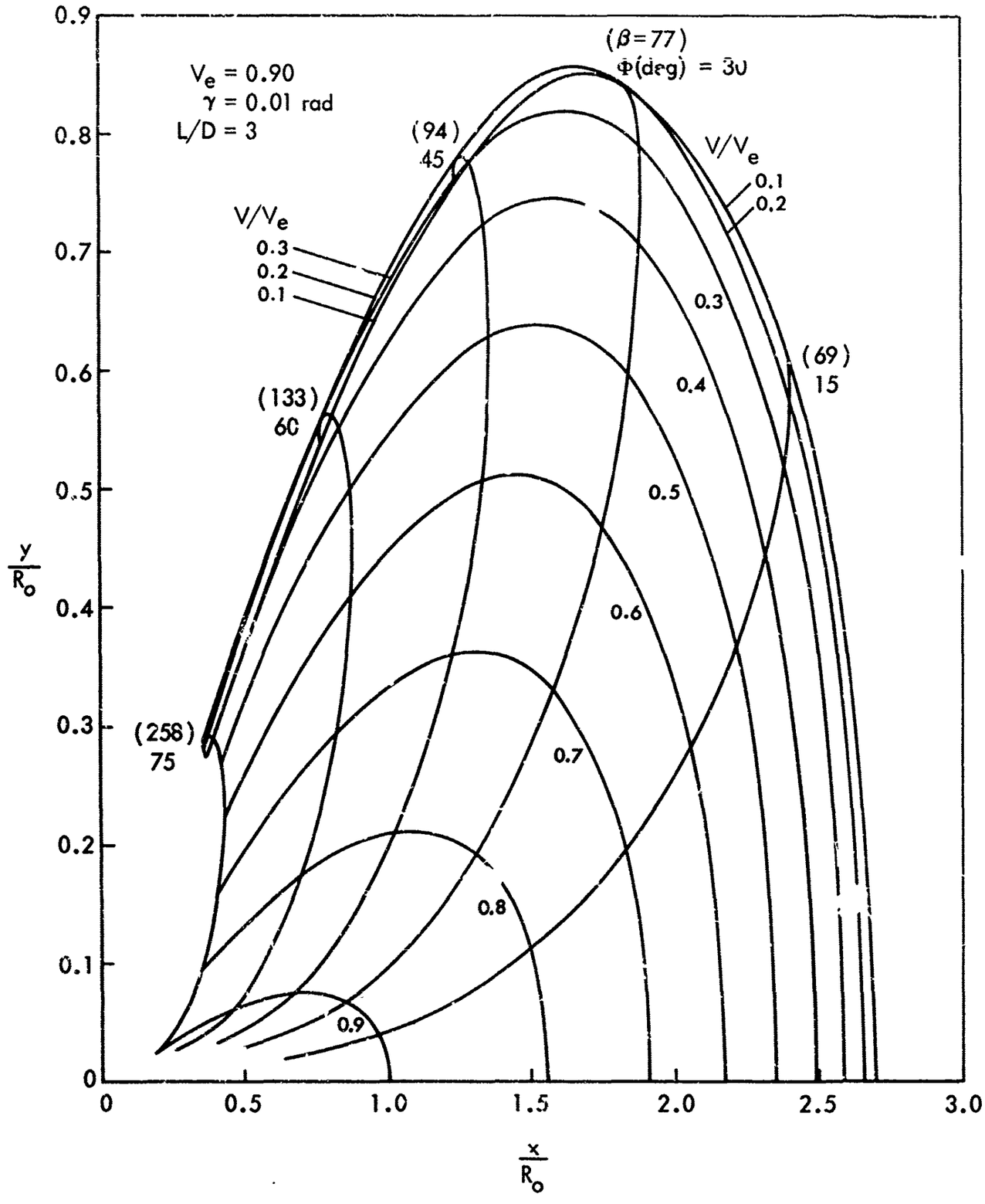

Fig. 9e— Influence of bank angle on ground trace
(L/D = 3, V_e = 0.90)
(Eqs. (29), (32))

The altitude and turn-angle relation as obtained from Eq. (22) is shown in Figs. 5a through 5e. As expected, the turn angle increases with increasing bank angle and the turning rate is highest at the end of a turn for constant bank angle. A comparison of Figs. 5b and 5d shows that for given flight conditions, the turn angle is larger for a small flight-path angle. Figures 5b and 5e show that for fixed β, bank angle, flight-path angle, and velocity ratio, the lower-entry-velocity vehicle will achieve a given turn angle at higher altitude. As mentioned previously, neglecting the lateral centrifugal term in the equations of motion may result in a higher turn-angle prediction. This error can be 30 percent, as pointed out by Wang[13] for the severe conditions he employed.

Equation (24) can be rewritten as

$$\frac{t}{u_o} g\gamma\sqrt{\beta(\beta - 2)} = \ell n \frac{[V\sqrt{\beta} - \sqrt{\beta - 2}][V_e\sqrt{\beta} + \sqrt{\beta - 2}]}{[V\sqrt{\beta} + \sqrt{\beta - 2}][V_e\sqrt{\beta} - \sqrt{\beta - 2}]} \tag{24a}$$

But $\sqrt{\beta(\beta - 2)} \approx \beta$ for large values of β, hence

$$\frac{t}{u_o} g\gamma\sqrt{\beta(\beta - 2)} \approx \frac{2gt}{u_o \frac{L}{D} \cos \Phi} \tag{24b}$$

The flight times for various flight conditions as given by Eq. (24) are plotted in Fig. 6. Substituting Eq. (24b) into Eq. (24a) shows that t is proportional to L/D cos Φ. In other words, the time decreases to zero as the bank angle approaches 90 deg or L/D approaches zero. It is evident that high-entry-speed and high-L/D vehicles require a longer time to slow down to the same speed ratio. For a bank angle equal to 90 deg, the equations are not applicable, since the flight path would resemble a ballistic trajectory rather than a lifting trajectory.

The flight-path length, S, for two different flight-path angles, $\gamma = 0.01$ and 0.02, is shown in Figs. 7a and 7b, which indicate that more than half of the distance to be flown will be in the region

where the flight speed is greater than 90 percent of the entry speed. In general, the flight-path length increases with increasing L/D at a given speed ratio.

As expected, if mean value $\bar{\gamma}$ is used, the flight-path length is a linear function of altitude, as given by Eq. (26) and shown in Fig. 8. It can be seen that the flight-path length would be doubled whenever the flight-path angle is reduced by approximately half.

The longitudinal and lateral ranges for constant-bank-angle flight are given by Eqs. (28) or (29) and (31) or (32), respectively. The numerical results for L/D = 1, 2, 3, and 4, and V_e = 0.98 and 0.90, are presented in Figs. 9a through 9e. It is clear that large ranges can be achieved by increasing L/D. The maximum lateral range can be obtained with a bank angle of about 43 deg at L/D = 1 and V_e = 0.98. However, this bank angle for maximum lateral range shifts to about 33 deg at L/D = 3 at low speed. The vehicle with high L/D (> 3) will proceed along its spiralling course far enough to achieve large heading changes and will be capable of reversing its direction of flight as it reaches very low speed. At a given speed ratio, both longitudinal and lateral ranges are very sensitive to the initial entry speed. A comparison of Figs. 9c and 9e shows that for γ = 0.01 and L/D = 3, a reduction of entry speed from 0.98 u_o to 0.90 u_o may reduce the longitudinal range by more than half and may cut the lateral range by more than one-third by the time the speed ratio of 0.1 is reached.

A comparison of equilibrium-glide results obtained in Ref. 12 (based on the assumptions of a very small flight-path angle) and those of the present analysis (based on the small and slowly changing flight-path angle of γ = 0.01 rad) is given in Table 1 and Fig. 10. These show that the assumption of a very small flight-path angle results in a smaller range prediction particularly for the lateral range of high-L/D vehicles, and in prediction of a larger bank-angle requirement for maximum lateral range.

One of the results of this study is a closed-form solution for predicting the performance of equilibrium-glide vehicles more accurately than was possible in the past without machine programming of the equations of motion directly. It can be concluded that for

Table 1

EFFECT OF L/D AND FLIGHT-PATH ANGLE ON LONGITUDINAL AND LATERAL RANGES[a]
($V_e = 0.98$, $V = 0.2V_o$)

L/D	γ (rad)	y_{max} (n mi)	$\frac{y_{\gamma\approx0.01}}{y_{\gamma\approx0}}$	x at y_{max} (n mi)	$\frac{x_{\gamma\approx0.01}}{x_{\gamma\approx0}}$	ϕ at y_{max} (deg)	$\frac{\phi_{\gamma\approx0.01}}{\phi_{\gamma\approx0}}$
1	0.01	580	1.068	4,197	1.119	42	0.933
	≈0	543		3,750		45	
2	0.01	2,236	1.171	9,080	1.187	38	0.927
	≈0	1,910		7,650		41	
3	0.01	4,780	1.292	14,450	1.290	33	0.892
	≈0	3,700		11,200		37	
4	0.01	8,940	1.277	28,550	1.818	27	0.871
	≈0	7,000		15,700		31	

[a]Based on assumptions of a very small flight-path angle ($\gamma \approx 0$) and a small and slowly changing flight-path angle ($\gamma \approx 0.01$ rad). Data for $\gamma \approx 0$ were obtained from Ref. 12.

orbital-speed reentry, a vehicle with L/D = 3, gliding at a flight-path angle of 0.01 rad and a constant bank angle of about 33 deg, can provide a reasonable lateral range greater than the earth's radius. In addition, more than half the longitudinal range will be achieved before the flight speed reaches 90 percent of the reentry velocity. However, half the lateral range will be achieved when the vehicle velocity is approximately 60 percent of the reentry velocity for L/D = 1, and 70 percent for L/D = 3, at optimum bank angle.

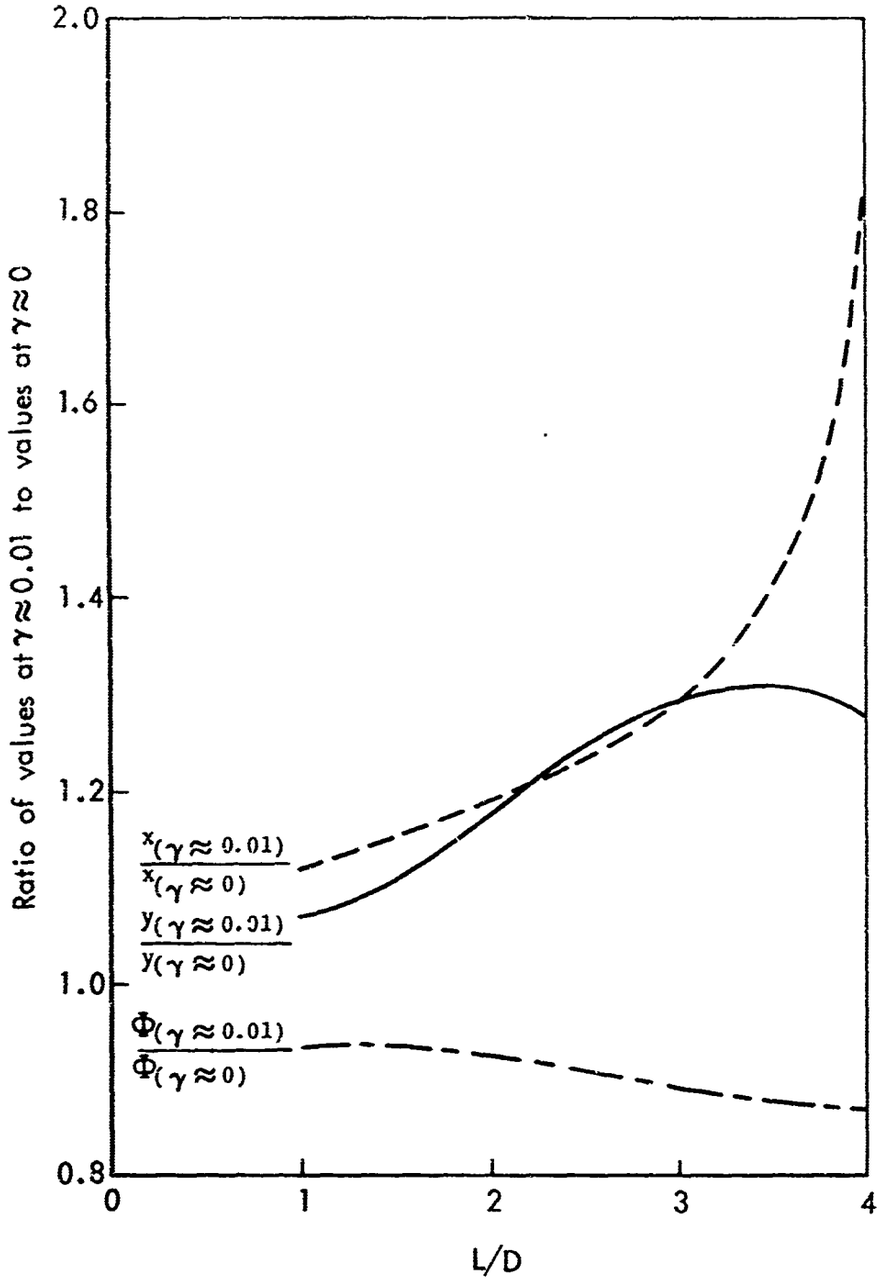

Fig. 10—Comparison of equilibrium-glide results

REFERENCES

1. Gazley, Carl, Jr., Deceleration and Heating of a Body Entering a Planetary Atmosphere From Space, The RAND Corporation, P-955, February 18, 1957; also published in Vistas in Astronautics, Pergamon Press, Ltd., London, 1958.

2. Gazley, Carl, Jr., Atmospheric Entry, The RAND Corporation, P-2052, July 15, 1960; also published in Handbook of Astronautical Engineering, McGraw-Hill Book Company, Inc., New York, 1961.

3. Eggers, Alfred, J., H. Julian Allen, and Standford E. Neice, A Comparative Analysis of the Performance of Long-Range Hypervelocity Vehicles, NACA TN 4046, October 1957.

4. Chapman, D. R., An Approximate Analytical Method for Studying Entry into Planetary Atmospheres, NACA TN 4276, May 1958.

5. Lees, L., F. W. Hartwig, and C. B. Cohen, "Use of Atmospheric Lift During Entry into the Earth's Atmosphere," ARS J., Vol. 29, No. 9, September 1959, pp. 633-641.

6. Loh, W.H.T., "Dynamics and Thermodynamics of Re-entry," J. Aero. Sci., Vol. 27, No. 10, October 1960, pp. 748-762.

7. Arthur, P. D., and H. K. Karrenberg, "Atmospheric Entry With Small L/D," J. Aero. Sci., Vol. 28, No. 4, April 1961, pp. 351-352.

8. Loh, W.H.T., "A Second Order Theory of Entry Mechanics into a Planetary Atmosphere," J. Aero. Sci., Vol. 29, No. 10, October 1962, pp. 1210-1221, and p. 1237.

9. Loh, W.H.T., "Some Exact Analytical Solutions of Planetary Entry," AIAA J., Vol. 1, No. 4, April 1963, pp. 836-842.

10. Cohen, M. J., Some Closed Form Solutions to the Problem of Re-entry of Lifting and Non-Lifting Vehicles, AIAA Paper No. 65-46, January 1965.

11. Loh, W.H.T., Extension of the Second Order Theory of Entry Mechanics to Circular and Supercircular Oscillatory-Type Entry Solutions, AIAA Paper No. 65-45, January 1965.

12. Nyland, F. S., Hypersonic Turning With Constant Bank Angle Control, The RAND Corporation, RM-4483-PR, March 1965.

13. Wang, H. E., Approximate Solutions of the Lateral Motion of Re-Entry Vehicles During Constant Altitude Glide, Aerospace Corporation, Report No. TDR-169 (3560-10) TN1, February 25, 1963 (to be published in AIAA Journal).

DOCUMENT CONTROL DATA

1. ORIGINATING ACTIVITY	2a. REPORT SECURITY CLASSIFICATION
THE RAND CORPORATION	UNCLASSIFIED
	2b. GROUP

3. REPORT TITLE

THE LONGITUDINAL AND LATERAL RANGE OF HYPERSONIC GLIDE VEHICLES WITH CONSTANT BANK ANGLE

4. AUTHOR(S) (Last name, first name, initial)

Chen, S. Y.

5. REPORT DATE	6a. TOTAL NO. OF PAGES	6b. NO. OF REFS.
January 1966	55	13

7. CONTRACT or GRANT NO.	8. ORIGINATOR'S REPORT NO.
AF 49(638)-1700	RM-4630-PR

9a. AVAILABILITY/LIMITATION NOTICES	9b. SPONSORING AGENCY
DDC 1	United States Air Force Project RAND

10. ABSTRACT

The Memorandum obtains approximate closed-form solutions for various flight conditions to determine the longitudinal and lateral range of hypersonic glide vehicles with a constant bank angle. Results for equilibrium-glide vehicles with constant lift-to-drag ratio and small, slowly changing flight-path angle are presented in graphic form. Other approximate closed-form solutions are obtained for glide re-entry at very small flight-path angle, near-constant-speed glide at high altitude, constant-deceleration glide at constant altitude, and constant-deceleration glide at fixed flight-path angle.

11. KEY WORDS

Hypersonic vehicles
Re-entry vehicles
Trajectories
Aerodynamics